

AperTO - Archivio Istituzionale Open Access dell'Università di Torino

Metabolomic adjustments in the orchid mycorrhizal fungus *Tulasnella calospora* during symbiosis with *Serapias vomeracea*

This is a pre print version of the following article:

Original Citation:

Availability:

This version is available <http://hdl.handle.net/2318/1744155> since 2021-01-23T19:39:54Z

Published version:

DOI:10.1111/nph.16812

Terms of use:

Open Access

Anyone can freely access the full text of works made available as "Open Access". Works made available under a Creative Commons license can be used according to the terms and conditions of said license. Use of all other works requires consent of the right holder (author or publisher) if not exempted from copyright protection by the applicable law.

(Article begins on next page)

Metabolomic adjustments in the orchid mycorrhizal fungus *Tulasnella calospora* during symbiosis with *Serapias vomeracea*

Andrea Ghirardo¹†, Valeria Fochi^{2,3}†, Birgit Lange¹, Michael Witting⁴, Jörg-Peter Schnitzler¹, Silvia Perotto^{2,3*}, Raffaella Balestrini^{3*}

¹Research Unit Environmental Simulation (EUS), Institute of Biochemical Plant Pathology, Helmholtz Zentrum München, Ingolstädter Landstr. 1, 85764, Neuherberg, Germany.

²Department of Life Sciences and Systems Biology, University of Turin, Viale Mattioli 25, 10125, Torino, Italy.

³National Research Council, Institute for Sustainable Plant Protection, Viale Mattioli 25, 10125, Torino, Italy.

⁴Research Unit Analytical BioGeoChemistry, Helmholtz Zentrum München, Ingolstädter Landstr. 1, 85764, Neuherberg, Germany.

†These authors contributed equally to this work

*Corresponding authors:

Raffaella Balestrini

Tel: +39 011 6502927

Email: raffaella.balestrini@ipsp.cnr.it

Silvia Perotto

Tel: +39 011 6705987

Email: silvia.perotto@unito.it

Concise and informative title:

Metabolomic adjustments during orchid mycorrhizal symbiosis

SUMMARY

- All orchids rely on mycorrhizal fungi for organic carbon, at least during early development. Orchid seed germination leads in fact to the formation of a protocorm, a heterotrophic postembryonic structure colonized by intracellular fungal coils, thought to be the site for nutrients transfer. The molecular mechanisms underlying mycorrhizal interactions and metabolic changes induced by this peculiar symbiosis in both partners remain mostly unknown.
- We studied plant-fungus interactions in the mycorrhizal association between the Mediterranean orchid *Serapias vomeracea* and the basidiomycete *Tulasnella calospora* using non-targeted metabolomics. Plant and fungal metabolomes obtained from symbiotic structures were compared with those obtained under asymbiotic conditions.
- Symbiosis induced profound metabolomic alterations in both partners. In particular, structural and signaling lipid compounds sharply increased in the external fungal mycelium growing near the symbiotic protocorms, whereas chito-oligosaccharides were identified uniquely in symbiotic protocorms.
- This work represents the first description of metabolic changes occurring in orchid mycorrhiza. These results - supported by transcriptomic data - provide novel insights on the mechanisms underlying the orchid mycorrhizal association and open intriguing questions on the role of fungal lipids in this symbiosis.

Keywords: metabolomics, orchid mycorrhiza, *Serapias*, symbiosis, transcriptomics, *Tulasnella calospora*

INTRODUCTION

In nature, most land plants associate with symbiotic fungi to form mycorrhizae. Depending on the morphology of the association and the taxonomic position of the symbiotic partners, four major mycorrhizal types are formed, namely arbuscular, ecto-, ericoid and orchid mycorrhiza. Mycorrhizal fungi increase the host plant's ability to acquire mineral nutrients and to tolerate biotic and abiotic stresses. In exchange, the fungal partner receives photosynthesis-derived carbon (C) as energy source and takes advantage of a protected niche (Smith & Read, 2008). Orchids are peculiar because their minute seeds lack an endosperm and the symbiotic fungus provides the germinating seed and developing embryo with organic C, a strategy termed myco-heterotrophy (Leake, 1994), as well as other nutrients such as N and P (Cameron *et al.*, 2006, 2007, 2008; Dearnaley & Cameron, 2017). Symbiotic seed germination leads to the formation of a heterotrophic orchid structure called protocorm (Rasmussen, 1995), in which intracellular hyphal coils (or *pelotons*) are formed and are thought to be responsible for the transfer of nutrients from the fungus to the host plant (Peterson & Farquhar, 1994). In the last years, the molecular bases underlying such peculiar plant-microbe interaction have been investigated (Yeh *et al.*, 2019). Gene expression profiling has identified fungal and plant genes putatively involved in signaling, symbiotic seed germination, mycoheterotrophy and plant defense (Zhao *et al.*, 2013; Perotto *et al.*, 2014; Kohler *et al.*, 2015b; Miura *et al.*, 2018; Lallemand *et al.*, 2019). Additionally, labeling experiments with stable isotopes (Cameron *et al.*, 2008; Kuga *et al.*, 2014) and molecular analyses (Zhao *et al.*, 2013; Fochi *et al.*, 2017a) have focused on the nutrient exchanges between the symbionts. Metabolomics is an alternative approach to investigate metabolic changes in symbiosis. Through the determination of the low-molecular-weight complement of biological systems (Kluger *et al.*, 2015), metabolomics provides direct information on the biochemical status of cells. Although little is known on metabolite alterations in orchid mycorrhiza (OM), some plant secondary metabolites may play a role in the interaction. For example, the amount of lusianthrin, an antifungal stilbenoid initially identified in the orchid *Lusia indivisa* (Majumder & Lahiri, 1990), was found to be strongly increased in protocorm-like bodies of *Cypripedium macranthos* colonized by the mycorrhizal fungus, suggesting a role in plant defense (Shimura *et al.*, 2007). Similarly, symbiotic *Anacamptis morio* protocorms showed a higher concentration of the phytoalexin orcinol as compared to non-mycorrhizal protocorms (Beyrle *et al.*, 1995). Chang & Chou (2007) found that the content of some metabolites (i.e., flavonoids, polyphenols, ascorbic acids, and polysaccharides) increased in mycorrhizal orchids, as compared to non-mycorrhizal plants.

Non-targeted metabolomics - i.e., a hypothesis-free analysis that aims to investigate the entire metabolome - represents a powerful tool to profile thousands of metabolites, especially in combination with pathway analyses (Fiehn *et al.*, 2000; Aharoni *et al.*, 2002; Schliemann *et al.*, 2008; Kårlund *et al.*, 2015). It has already been used to investigate plant-microbe interactions in legume root nodules (Zhang *et al.*, 2012), ectomycorrhizae (Tschapinski *et al.*, 2014) and arbuscular mycorrhizae (Schliemann *et al.*, 2008; Laparre *et al.*, 2014; Rivero *et al.*, 2015). Here, we employed non-targeted metabolomics to investigate *in vitro* the mycorrhizal association between the Mediterranean orchid *Serapias vomeracea* and the basidiomycete *Tulasnella calospora* (Cantharellales). In particular, *S. vomeracea* seeds and *T. calospora* mycelium were grown together to form mycorrhizal orchid protocorms, and plant and fungal metabolite profiles were compared to those obtained when plant and fungus were cultivated separately as asymbiotic protocorms and free-living mycelium. We integrated metabolomic analyses with genomic information available for *T. calospora* (Kohler *et al.*, 2015a) and our published transcriptomic data (Fochi *et al.*, 2017a). In addition to differences in the metabolite profiles of symbiotic and asymbiotic protocorms, the results revealed intriguing and unexpected differences in the lipid content of free-living and symbiotic *T. calospora* mycelium.

MATERIAL AND METHODS

Biological materials

Free-living mycelium of *T. calospora*

Tulasnella calospora (AL13 isolate) mycelium was originally isolated from mycorrhizal roots of the terrestrial orchid species *Anacamptis laxiflora* in Northern Italy (Girlanda *et al.*, 2011) and was grown on solid 2% Malt Extract Agar (MEA) at 25°C for 20 days before use. Three plugs (6 mm diameter) of actively growing *T. calospora* mycelium were transferred onto a sterilized cellophane membrane placed on top of Oat Agar (OA, 0.3% milled oats, 1% agar; Fig. 1a, d), the same used for symbiotic seed germination, in 11 cm *Petri* dishes (Schumann *et al.*, 2013). After 20 days at 25°C, the free-living mycelium (FLM) was collected, immediately frozen in liquid N₂ and stored at -80°C.

Symbiotic and asymbiotic germination of *Serapias vomeracea* seeds

Symbiotic seed germination was obtained by co-inoculation of mycorrhizal fungus and orchid seeds in 9 cm *Petri* dishes, as previously described in Ercole *et al.* (2015). After surface sterilization, seeds were resuspended in sterile water and dropped on strips of autoclaved filter paper (1.5 x 3 cm) positioned on solid oat medium (0.3% (w/v) milled oats, 1% (w/v) agar). A plug of actively growing *T. calospora* mycelium was then placed in the center of each *Petri* dish and plates were incubated at 20°C in full darkness for 30 days (Fig. **1b**). Asymbiotic germination was obtained by placing surface-sterilized seeds directly on modified BM1 culture medium (Van Waes & Debergh, 1986) at 20°C in darkness. Symbiotic protocorms (SYMB) were collected 30 days post-inoculation (dpi) and asymbiotic protocorms (ASYMB) 120 dpi. Symbiotic germination was performed by placing the mycelial plug on autoclaved cellophane membrane, in order to collect the fungal mycelium (MYC) growing near to the protocorms (Fig. **1c-d**). MYC samples were harvested by carefully scraping the mycelium with a spatula. All samples were flash-freezed in liquid N₂ and stored at -80 °C.

Sample preparation for metabolomic analysis

S. vomeracea symbiotic and asymbiotic protocorms and *T. calospora* mycelium were disrupted with TissueLyser (18Hz, 2 min, twice). Frozen powder samples (100 mg) were extracted with 1 ml of methanol:isopropanol:water (1:1:1, v/v) for 1 h at 4°C in constant shaking. Successively, the solution was centrifuged at 14,000 rpm for 15 min at 4°C and the supernatant was recovered, dried in a centrifugal evaporator (SpeedVac, Savant Inc, USA) and stored at -80°C. Before metabolomic analysis, the dried samples were dissolved in 200 µl of 50% acetonitrile in water and centrifuged at 14,000 rpm at 4°C for 10 min.

UPLC-UHR-QqToF-MS measurements

Ultra Performance Liquid Chromatography (UPLC) Ultra-High Resolution (UHR) tandem quadrupole/Time-Of-Flight (QqToF) mass spectrometry (MS) measurements were performed on an Ultimate 3000RS (ThermoFisher, Bremen, Germany) coupled to a Bruker Impact II with Apollo II source (ESI source) (Bruker Daltonic, Bremen, Germany). Chromatographic separation was achieved on a C₁₈ column (100 mm x 2.1 mm inner diameter with 1.7 µm particles, Fortis Technologies - Clayhill Industrial Park Neston Cheshire, UK). Eluent A was water with 0.1% of formic acid and eluent B was acetonitrile with 0.1% of formic acid. Gradient elution started with an initial isocratic hold of 0.5% B for 1 min, followed by an increase to 30% B in 15 min and a further increase to 80% B for 5 min. During the last 3 min, the initial conditions of 0.5% B were restored. The flowrate was 400 µl min⁻¹ and the column

temperature was continuously maintained at 40°C. The auto-sampler temperature was set to 4°C. For each sample, two technical replicates were measured in both positive (+) and negative (-) ionization modes. Prior to sample analyses, quality control (QC) samples prepared from the aliquots of the different samples were injected for column conditioning. Mass calibration was achieved with 50 ml of water, 50 ml isopropanol, 1 ml sodium hydroxide, and 200 µl formic acid. The MS was operated under the following conditions: the nebulizer pressure was set to 2 bar, dry gas flow was 10 l min⁻¹, dry gas temperature was 220°C, a capillary voltage was set to 4000 V for the (+) and 3000 V for the (-) ionization mode and the endplate offset was 500 V. Mass spectra were acquired in a mass range of 50-1300 m/z in both (±) modes.

Non-targeted metabolomic analysis

Each MS spectrum file was separately imported into the GeneData Expressionist for MS software v13.5 (München, Germany) for peak peaking and alignment. The spectra were pre-processed by the following steps: i) chemical noise reduction, ii) retention time (RT) alignment, iii) identification of m/z features using the summed-peak-detection feature implemented in the GeneData software, iv) peaks not present in at least 10% of the mass spectra were discarded for isotope clustering, v) singletons (clusters with only one member) were discarded. The resulting peak matrix was exported, both (±) modes were combined, and the average peak intensity of both technical replicates was calculated and further used for statistical and annotation analyses. Mass features (m.f.) appearing in less than 75% of the biological replicate were removed from the data matrix. The resulting peak list was further used for annotation and statistical analysis. Metabolic annotation was achieved as before (Way *et al.*, 2013; Kersten *et al.*, 2013) using the portal MassTRIX3 (<http://masstrix3.helmholtzmuenden.de/masstrix3/>). Compared to MassTRIX (Suhre & Schmitt-Kopplin, 2008; Wägele *et al.*, 2012), the updated version of MassTRIX3 contains all metabolites of KEGG (<http://www.genome.jp/kegg/>), the Human Metabolome Database (HMDB - <http://www.hmdb.ca>), ChemSpider (<http://www.chemspider.com>), KNApSAcK (<http://kanaya.naist.jp/KNApSAcK/>), Lipidmaps (<http://www.lipidmaps.org/>) and PubChem (<https://pubchem.ncbi.nlm.nih.gov/>). Log2 ratios of m.f. intensities (log2) were calculated for SYMB/ASYMB, SYMB/MYC, SYMB/FLM, and MYC/FLM to visualize metabolic up- or down-regulation. Putative molecular formulas were calculated from all m.f. using 4 ppm as a threshold. Molecular formulas were used to calculate H/C, O/C, N/C, P/C, S/C, N/P ratios for

the production of van Krevelen diagrams and for the multidimensional stoichiometric compound classification (MSCC) (Rivas-Ubach *et al.*, 2018).

Pathway and Functional analyses

Pathway analysis was performed by using the Pathway Omics Dashboard tools of BioCyc (<https://biocyc.org/>) (Paley *et al.*, 2017) on annotated metabolites, the concentrations of which changed significantly in MYC/FLM. We used MetaCyc v23.1 (<https://Metacyc.org>) as reference database (Caspi *et al.*, 2018). The biological function of the up/downregulated annotated metabolites in MCY/FLM were obtained from the KEGG, HMDB and Lipid Maps databases.

Transcriptomic data

Symbiotic and asymbiotic growth conditions used for these metabolomic studies were the same previously investigated by transcriptomics in Fochi *et al.* (2017a). Transcriptomic data are, however, missing for the MYC samples. The complete series of fungal and plant transcripts are available at GEO (GSE86968 and GSE87120, respectively).

Statistical analysis

Experiments were performed using four independent biological replicates. Metabolomic data were analyzed using Principal Component Analysis (PCA) and Orthogonal Partial Least Squares Regression (OPLSR) (SIMCA-P v13, Umetrics, Umeå, Sweden). The pre-processing of the data followed established procedures (Ghirardo *et al.*, 2005, 2012, 2016). Discriminant masses (Kaling *et al.*, 2015) between the different mycelia (MYC and FLM) and the protocorms (SYMB and ASYMB) were further tested for statistical significance using a false discovery rate (FDR) of 5% as previously described (Way *et al.*, 2013).

RESULTS

Impact of symbiosis on plant and fungal metabolomes

The metabolome of symbiotic protocorms (SYMB) and *T. calospora* mycelium (MYC) collected near the symbiotic protocorms (Fig. **1a-b**) were compared with asymbiotic protocorms (ASYMB) and free-living mycelium (FLM) grown in pure culture on the same medium used for symbiotic seed germination (Fig. **1c-d**). We revealed a total of 24818 metabolite-related mass features (m.f.), with the plant metabolome being more complex

(14722 m.f. for SYMB, 16213 for ASYMB) than the fungal metabolome (4376 m.f. for MYC, 3337 for FLM).

The number of common and specific m.f. in symbiotic and asymbiotic plant samples and mycelia is visualized in the Venn diagram (Fig. 2). The 521 m.f. common to all samples are most likely related to a “core metabolome” composed of primary metabolites found in both partners (Fig. 2). A relatively high number of m.f. (1265) was found in MYC samples but not in FLM ones, indicating accumulation of distinct metabolites in the fungal hyphae close to (but outside) the host plant. We found an overlapping metabolome composed of 8583 m.f. in SYMB and ASYMB orchid protocorms, but not in MYC or FLM samples, likely representing plant metabolites involved in general plant functions. Several m.f. were unique to symbiotic (SYMB, 3977) or asymbiotic (ASYMB, 5433) orchid protocorms. Although some of these unique m.f. likely represent plant metabolites regulated by symbiosis, some may be due to the different culture media required to obtain symbiotic and asymbiotic protocorms.

Metabolites uniquely found in MYC and SYMB samples (291 m.f.) or in MYC, SYMB, and FLM samples (315 m.f.) likely represent fungus-specific compounds, as they were not found in ASYMB samples. In addition, some unique metabolites in SYMB samples could originate from the mycorrhizal fungal partner colonizing symbiotic protocorm tissues. Indeed, fungal metabolites uniquely produced in symbiosis would group together with the SYMB-specific metabolites (Fig. 2).

In addition to unique and shared plant and fungal metabolites, the symbiotic plant-fungus interaction likely resulted in up- and downregulation of a broader set of metabolites. PCA of all m.f. abundances comprehensively visualized changes in metabolite levels and showed a highly diverse metabolic profile among samples (Fig. 3). Not surprisingly, the most considerable distance (46%), as seen by the first component (PC1), was between plant protocorms (ASYMB/SYMB) and fungal mycelium (MYC/FLM). A further and significant distance among data was described by PC2 (34%), which clearly separated SYMB from ASYMB samples and, to a lesser extent, by PC3 (7%), MYC from FLM samples.

To gain insights into metabolites and metabolic pathways altered in the symbiosis, we performed an OPLSR analysis on the m.f., followed by database annotation of the discriminant masses (Kersten *et al.*, 2013). By doing so, we putatively annotated the m.f. that characterized the following sample pairs: SYMB/ASYMB, SYMB/MYC, SYMB/FLM, and MYC/FLM (Table S1). Additionally, we classified compounds based on their elemental compositions using the very recently developed multidimensional stoichiometric compound

classification (MSCC) approach (Rivas-Ubach *et al.*, 2018). This method avoids the limitations of actual database coverage, especially for less described organisms. Using MSCC in combination with van Kreveln diagrams, we visualized the significant global metabolic changes of the main compound categories (i.e., lipids, protein-related, amino sugars, carbohydrates, nucleotides, and phytochemical compounds) up/downregulated during plant-fungus symbiosis (Fig. 4). MSCC analysis highlighted the high abundance of lipids in MYC samples, as compared to FLM samples (Fig. 4a). The increased levels of lipids in MYC samples can also be seen in the van Krevelen diagram, where compounds with H/C ratio ≥ 1.32 and O/C ratio ≤ 0.6 were strongly upregulated (Fig. 4c). Conversely, phytochemical compounds were downregulated in the MYC/FLM comparison (Fig. 4a). Importantly, carbohydrates (O/C ratio ≥ 0.8 and $1.65 \leq \text{H/C} < 2.7$) were lower in MYC samples, indicating either a shift from carbohydrate metabolism to, for instance, lipid metabolism, or perhaps C transfer towards the mycorrhizal plant protocorms. The latter hypothesis would agree with the carbohydrates increase in SYMB protocorms (Fig. 4b, d).

Functional enrichment analysis in *T. calospora*

Metabolic changes caused by symbiosis were clearly detected in the external hyphae of *T. calospora* (Fig. 4a) and represent an aspect of the interaction so far unexplored. We first used the Pathway Omics Dashboard tool of MetaCyc as unbiased analysis to visualize the overall metabolic changes of this fungus during its symbiotic interaction with the plant. When compared to FLM, the MYC metabolome was highly enriched in compounds involved in the synthesis of lipids, followed by cell-structures, hormones, carbohydrates, or compounds involved in metabolic regulation (Fig. 5). Conversely, cumulative changes in metabolites involved in secondary metabolism were found to be strongly downregulated in MYC samples, as compared to FLM.

Since MetaCyc was unable to classify ~70% of the annotated metabolites, we additionally investigated the chemical taxonomy and functions of regulated metabolites using data from the literature or available databases. This in-depth analysis showed that several compounds related to cell-structure and signaling were increased in MYC samples (Fig. 6, Table S1). ‘Lipids’ were still the most upregulated compounds in the external mycelium of *T. calospora*. Notable changes were also observed in several nitrogen-, oxygen- and sulfur-containing compounds (Fig. 6a). With respect to functions, symbiosis caused an overall increase in the amount of structural, signaling, and energy-related compounds in MYC samples, as compared to FLM samples, mainly related to lipids (Fig. 5-6b, Table S1). Among lipids (120

metabolites), the glycerophospholipids (68), fatty acyls (FA) (14) and isoprenoids (prenol lipids) (13) were strongly upregulated in MYC samples ($\log_2 > 10$) (Table S1). Some nitrogen-containing organic compounds (29), organosulfur compounds (8), and phytochemical metabolites (14) involved in defense were also highly upregulated in MYC samples. On the other hand, fewer lipids (48) (FA, 10; isoprenoids, 9), but more nitrogen-containing organic compounds (41), organosulfur compounds (17), and, among phytochemical compounds (17), alkaloids (14) were significantly downregulated (Fig. 6).

The external mycelium of *T. calospora* showed specific changes in lipid content

The sharpest metabolomic differences between MYC and FLM samples were in the levels and compositions of lipids, in particular glycerophospholipids (GPL) and sphingolipids (Fig. 6, S1, Table S1). Among 81 significantly upregulated GPL in MYC samples, the most upregulated GPL ($\log_2 = 21.4$) was putatively annotated as lysophosphatidylethanolamine (LysoPE), a lipid metabolite involved in signaling. Notably, 18 glycerophosphoserines (GPS) were found to be strongly ($\log_2 > 10$) upregulated, as compared to only one being downregulated, and the abundance of the GPL precursor palmitic acid was consistently increased ($\log_2 = 9.1$). Among GPL, 13 phosphatidylcholines (PCs) and 9 phosphoinositides (PIs) were more abundant ($\log_2 > 10$) in MYC samples than in FLM samples. Also, a glycerophosphocholine, putatively annotated as 1-palmitoyl-sn-glycero-3-phosphocholine (LPC(16:0)) was upregulated ($\log_2 = 14.4$) in MYC samples. An essential intermediate in the biosynthesis of both triacylglycerols and GPL, and therefore involved in energy (storage and source) and structural metabolism, was the GPL phosphatidic acid PA(22:0/14:1(9Z)), also upregulated ($\log_2 = 12.9$) in MYC samples. Highly upregulated in MYC samples were also the FA derivative of hydroxyeicosatetraenoic acid, 15-HETE ($\log_2 = 21$), and the 8-hydroxyoctadeca-9Z,12Z-dienoic acid (8-HODE or laetisarinic acid) ($\log_2 = 13.85$), a FA having allelochemical functions. Moreover, the strong accumulation of sphingosine ($\log_2 = 13.58$) and PI-Cer(d20:0/16:0) ($\log_2 = 12.58$) indicate an increase in sphingolipid biosynthesis in MYC samples.

Direct integration of metabolomic and transcriptomic data was unfortunately not possible because previous transcriptomic analyses (Perotto *et al.*, 2014; Fochi *et al.*, 2017a) did not investigate the MYC condition. However, significant changes in the expression of fungal genes involved in lipid metabolisms (Table S2) were observed between SYMB and FLM samples. Among the annotated fungal genes most upregulated in symbiosis (fold change, 'FC' > 10) were two members of the Ca^{2+} -independent phospholipase A₂ (Protein ID (#)

53822, #25657) and a myo-inositol-1-phosphate synthase (#72491), an essential enzyme for the biosynthesis of inositol containing phospholipids (PIs) and certain sphingolipid signaling molecules. Two fungal genes corresponding to phosphoinositide kinases (FC=4.6, # 26793, FC=2.4, # 28485) and three sphingosine N-acyltransferases, a key enzyme involved in sphingolipid biosynthesis, were upregulated in symbiosis (#18228, #79587, #18227) (Table S2). Conversely, a glucosylceramidase (#33445) was strongly downregulated. Several genes involved in FA metabolism through the Acyl-CoA coenzyme were also affected (Table S2), including two down-regulated genes coding for thiolases (#16280, #131995). Finally, we observed large changes of 29 isoprenoids in the MYC/FLM comparison (Table S1). Eight triterpenoids, one diterpene, and one tetraterpene were strongly upregulated (log2 >10). Although transcriptional information on the MYC condition is not available, 5 *T. calospora* genes encoding terpenoid synthases were significantly upregulated in symbiotic protocorms (Table S2), two of them with FC >20 (#70959, #22905).

Nitrogen-containing fungal compounds

Nitrogen-containing (non-phospholipids) compounds were the second group of metabolites significantly affected in *T. calospora*, with a high proportion downregulated in MYC samples, as compared to FLM (Fig. 6a, Table S1). Although most of these compounds could not be reliably annotated due to the constraints of the available databases, they indicate sharp changes in nitrogen metabolism in the fungus during symbiosis. Two of the few identified compounds with increased levels in MYC samples, as compared with FLM, were UDP-N-acetyl-D-glucosamine (UDP-GlcNAc) (log2=9.52) and dolichyl-N-acetyl-alpha-D-glucosaminyl-phosphate (log2=11.47), N-containing compounds essential for the biosynthesis of N-linked glycans, glycosylphosphatidylinositol (GPI)-anchored proteins, sphingolipids and glycolipids. UDP-GlcNAc can be polymerized to form chitin, a major component of the fungal cell wall. Short oligomers of chitin and chitosan, its deacetylated form, were found similarly enriched (log2 from 11.9 to 13.6) in SYMB when compared with either the MYC or the FLM samples, whereas no differences were observed between MYC and FLM samples (Table S1). Chitosan is produced through the activity of chitin deacetylase, and 3 chitin deacetylase genes (#174258, #26855, #107589), out of the 9 present in the *T. calospora* genome, were significantly upregulated in SYMB with respect to FLM (Table S2). By contrast, a single chitin synthase (#31299) was slightly upregulated in symbiosis (Table S2). Short chitin oligomers can be important signals in symbiosis and could also be generated from long chitin polymers by the activity of chitinases. The expression of both fungal and

plant chitinases was modified by symbiosis (Tables **S2-3**), some plant chitinases being strongly upregulated in symbiotic protocorms (TRINITY Contig Names: DN77284_c0_g1_i3, DN5745_c0_g1_i1, DN66370_c0_g1_i1, DN62020_c0_g1_i1).

Comparing symbiotic and asymbiotic conditions, another primary class of regulated nitrogen-containing compounds was involved in amino acid metabolisms (Table **S1**). Accumulation of N-L-argininosuccinate was found in SYMB when compared to all other samples ($\log_2 = 3.8$ with ASYMB; $\log_2 = 13.3$ with MYC and FLM). This compound is involved in arginine biosynthesis and fumarate formation, an essential intermediate of the TCA cycle. Unfortunately, the metabolomic study of symbiotic tissues (SYMB) is not an easy task because they contain both plant and fungal metabolites and assignment of most mass features to the symbionts is uncertain. Therefore, most amino acids and amino acid derivatives could not be assigned to the fungus or to the plant, with few exceptions. One was the putatively annotated ergothioneine, a naturally occurring metabolite of histidine exclusively found in some fungi and bacteria (Cumming *et al.*, 2018). The levels of ergothioneine were much higher in SYMB ($\log_2=11.35$) than in MYC or FLM. The levels of hercynine, another fungal-specific and histidine related compound, were by contrast low ($\log_2=-10.31$) in the SYMB vs MYC comparison. Transcriptomic evidence points to an important role of *T. calospora* in histidine biosynthesis during symbiosis, with three biosynthetic genes (#108905, #73648, #141375) being significantly upregulated in SYMB samples (Table **S2**).

Organosulfur compounds

Significant changes in sulfur-containing compounds were observed in *T. calospora* (Table **S1**), with 14 compounds being upregulated ($\log_2>10$) and 18 downregulated ($\log_2<-10$) in MYC samples, as compared to FLM. Similar to nitrogen-containing compounds, many organosulfur compounds could not be reliably annotated. An exception was S-adenosylmethioninamine, a decarboxylated derivative of S-adenosylmethionine (SAM) involved in polyamine biosynthesis (Pegg *et al.*, 1998). Notably, the amount of S-adenosylmethioninamine in MYC samples was sharply reduced ($\log_2 = -11.05$), as compared to FLM, whereas SAM amount was sharply increased ($\log_2 = 8.9$). SAM is a major source of methyl groups for reactions involving methylation. The substantial SAM accumulation in MYC samples (Table **S1**) suggests a role in symbiosis. Although SAM levels were similar in SYMB, MYC or FLM samples, transcriptomics revealed that the *T. calospora* SAM synthetase gene was upregulated ($FC=4.29$, #72837) in symbiosis (Table **S2**). Metabolomic

data further indicate a significantly lower ($\log_2=-10.3$) SAM content in SYMB as compared to ASYMB (Table S1), suggesting down-regulation of the plant SAM in symbiosis.

DISCUSSION

Transcriptomics is the most common approach to indirectly investigate metabolic changes in symbiotic organisms because it reveals the contributions of both partners through changes in their gene expression. This approach was successfully used to investigate orchid mycorrhizal (OM) protocorms, symbiotic structures that contain a mixture of plant and fungal molecules that cannot be separated before molecular or biochemical analyses (Zhao *et al.*, 2013; Fochi *et al.*, 2017a; Miura *et al.*, 2018). However, although gene regulation is indicative of activation or repression of distinct biosynthetic pathways, transcriptional regulation of genes encoding enzymes does not necessarily reflect the final enzymatic activity, and there may be no direct association between metabolites and transcripts (Cavill *et al.*, 2016). Therefore, we used a non-targeted metabolomic approach to investigate metabolic changes in OM, and transcriptomic data were only used to corroborate metabolomic results. Metabolomics yielded particularly interesting results when the external mycelium of the OM fungus *T. calospora* growing near to symbiotic *S. vomeracea* protocorms (MYC) was compared with the free-living mycelium. All organic nutrients needed by the developing mycoheterotrophic protocorms are thought to be provided by the symbiotic fungus in the OM symbiosis. Thus, the metabolites identified in the MYC samples are most likely produced by *T. calospora* and differentially accumulated in the presence of the plant.

Symbiosis caused profound changes in the lipid content of T. calospora

Lipids were the most prominent upregulated metabolites in the external *T. calospora* mycelium, as compared to asymbiotically-grown mycelium. Besides being major structural components of cell membranes, lipids provide critical biological functions as energy and carbon storage, in signaling, stress response and plant-microbe interactions (Siebers *et al.*, 2016). Lipids have recently become an important topic in mycorrhizal research because a substantial increase in the amount of lipids was discovered in the hyphae of arbuscular mycorrhizal (AM) fungi during symbiosis (Keymer *et al.*, 2017). AM fungi are obligate biotrophs that fail in the *de novo* biosynthesis of fatty acids but become enriched thanks to lipid transfer from the plant. This is unlikely the case for OM fungi because the *T. calospora* genome contains the genetic machinery for lipid biosynthesis, and the increased lipid content in the external *T. calospora* hyphae more likely reflects endogenous lipid biosynthesis.

427 Phospholipids and sphingolipids are vital components of cell membranes and play key roles
 428 in signaling, cytoskeletal rearrangement, and in membrane trafficking (Meijer & Munnik,
 429 2003; Michell, 2008; Fyrt & Saba, 2010; Balla, 2013; Hou *et al.*, 2016; Singh & Del Poeta,
 430 2016; Hannun & Obeid, 2018; Blunsom & Cockcroft, 2020). In fungi, sphingolipids are
 431 important for hyphae formation (Oura & Kajiwar, 2010), regulating cell growth and
 432 differentiation (Obeid *et al.*, 2002), and cell division (Epstein *et al.*, 2012). In addition, lipid-
 433 derived molecules are essential for intra- and extra-cellular signaling and for defense against
 434 the proliferation of undesired microbes (Hou *et al.*, 2016; Siebers *et al.*, 2016; Singh & Del
 435 Poeta, 2016; Wang *et al.*, 2020). Lipid peroxidation of free fatty acids, acyl groups of
 436 triacylglycerols or galactolipids, is commonly activated to induce defense against pathogens.
 437 For instance, oxylipins are essential in signal transduction and in both induced systemic
 438 resistance (Wang *et al.*, 2020) and systemic acquired resistance (Siebers *et al.*, 2016).

439 Overall, we observed a generally increased level of several structural lipid constituents of cell
 440 membranes, such as glycerophospholipids (GPL), fatty acyls (FA), glycerolipids,
 441 saccharolipids and some of their metabolic precursors (e.g. palmitic acid and UDP-GlcNAc).
 442 Palmitic acid is one of the most common saturated fatty acids found in animals, plants and
 443 microorganisms, and the first fatty acid produced during lipogenesis (Sidorov *et al.*, 2014;
 444 Carta *et al.*, 2017). UDP-GlcNAc, an essential precursor of the fungal cell wall chitin, is also
 445 involved in the biosynthesis of sphingolipids and sulfolipids (Bowman & Free, 2006; Furo *et al.*,
 446 2015; Ebert *et al.*, 2018). The most represented lipids upregulated in the external
 447 mycelium of *T. calospora* were GPL. Particularly, phosphatidylserines (PS) represented ca.
 448 41% of the up-regulated GPL compounds. PS are mostly restricted to the cytoplasmic
 449 membrane leaflet, and the covalent attachment of serine to the phosphate group creates a
 450 negative charge essential for targeting and functioning of several intracellular signaling
 451 proteins and for the activation of specific kinases, such as protein kinase C (Kay & Grinstein,
 452 2011). Sphingosine and PI-Cer(d20:0/16:0) are precursors of sphingolipids, also important
 453 components of fungal cell membranes (Meijer & Munnik, 2003; Hou *et al.*, 2016; Singh &
 454 Del Poeta, 2016). These compounds and other 9 PIs were strongly upregulated in the external
 455 *T. calospora* mycelium, likely reflecting the upregulation in symbiosis of phosphoinositide
 456 phosphatases and serine/threonine protein kinases, key enzymes involved in the biosynthesis
 457 of sphingolipids and glycerophosphoinositols (Balla, 2013; Hou *et al.*, 2016; Hannun &
 458 Obeid, 2018; Blunsom & Cockcroft, 2020).

Some membrane GPL also play essential roles in pathogenic and mutualistic interactions. For example, changes in membrane lipid compositions of rhizobia, including PS and PE, prevented the formation of nitrogen-fixing legume nodules (Vences-Guzmán *et al.*, 2008). In fungi, PS and PE have been correlated with *Candida albicans* virulence (Cassilly & Reynolds, 2018), and an increase in PS was observed during fungal differentiation in the phytopathogenic *Rhizoctonia solanii* (Hu *et al.*, 2017). Sphingolipids are also involved in plant-fungal interactions, and early intermediates of sphingolipid biosynthesis were found to be essential for normal appressoria development and pathogenicity of *Magnapothe oryzae* (Liu *et al.*, 2019).

In addition to structural membrane components, we found a strongly increased amount of lipids involved in signaling and defense in the external mycelium of *T. calospora*. The 1-18:1-lysophosphatidylethanolamine (LysoPE) belongs to the class of lysophospholipids, which serve essential signaling functions in plants and act as plant growth regulators (Meijer & Munnik, 2003; Cowan, 2006; Hou *et al.*, 2016). The FA 8-HODE (or laetisarinic acid) originates from linoleic acid and is a bioactive oxylipin acting as a communication signal in plant-fungus interactions (Brodhun & Feussner, 2011; Christensen & Kolomiets, 2011). 8-HODE was first discovered in the basidiomycete *Laetisaria arvalis* as an allelochemical that suppresses growth of phytopathogenic fungi (Bowers *et al.*, 1986). 15-HETE, the hydroxylated fatty acid substrate for the oxylipin biosynthesis, is an intermediate of sphingolipids, extracellular glycolipids apparently necessary for signaling. The strong upregulation of 8-HODE (log₂=13.8) and 15-HETE (log₂=21) in MYC samples, as compared to FLM, indicates that the signaling apparatus in MYC samples is highly active during symbiosis. Interestingly, some Ca²⁺ independent phospholipase A2 were among the most upregulated *T. calospora* genes (Table S2). This enzyme family plays important functions in membrane homeostasis, signal transduction, and virulence (Valentín-Berrios *et al.*, 2009).

Although we could hypothesize that the increased amount of structural membrane lipids in the fungal hyphae outside the mycorrhizal protocorm may simply reflect a stimulation of hyphal growth and a need for membrane biogenesis following symbiosis, the increase in potential membrane signaling molecules is intriguing. Also, several upregulated lipids in *T. calospora* contained phosphate, and it has been suggested by Plassard *et al.* (2019) that organic phosphate released by membrane lipids may be transferred to the plant in AM symbiosis. However, although organic phosphate transporters were identified in the genome of mycorrhizal fungi, including OM fungi (Plassard *et al.*, 2019), their occurrence in plants is to our knowledge unknown.

Nitrogen- and sulfur-containing organic compounds in the external *T. calospora* mycelium

Compared to lipids (see above), more difficult to explain is the large percentage of nitrogen and sulfur-containing compounds downregulated in the same MYC samples (Fig. 6). In our system, the OM fungus likely provides the host with organic nitrogen, as suggested by the strong upregulation of some plant amino acid transporters in the mycorrhizal protocorms cells (Fochi *et al.*, 2017a,b). We could, therefore, speculate that depletion of some nitrogen-containing compounds in the external MYC mycelium may be the result of N transfer to the host. It is also possible that some of those non-annotated upregulated compounds are simply involved in the metabolism of nitrogen-containing lipids, such as glycerophospholipids and sphingolipids.

About sulfur, there is currently no information on its transfer to the host plant in OM. Among the few sulfur-containing compounds that could be reliably identified, S-adenosyl-L-methionine (SAM) was upregulated in MYC samples. SAM is the major methyl group donor for the methylation of DNA, RNA, proteins, metabolites, or phospholipids (Mato *et al.*, 1997). Overexpression of SAM synthetase gene in *Aspergillus nidulans* had a substantial impact on development and secondary metabolism (Gerke *et al.*, 2012). Given the wide variety of target substrates of methyltransferases that use SAM as a methyl group donor, it is currently impossible to identify such targets in *T. calospora*.

Another notable sulfur and nitrogen-containing compound was ergothioneine (EGT) (Sheridan *et al.*, 2016). EGT occurs primarily in fungi, and no biosynthesis was detected so far in plants. Thus, it was possible to trace this compound in symbiotic protocorms, where it was highly induced ($\log_2=11.35$) as compared to external or free-living mycelium. Ergothioneine exhibits powerful antioxidant properties, and biosynthetic deficiency in *A. fumigatus* mutants indicates a role for growth at elevated oxidative stress conditions (Sheridan *et al.*, 2016). Its accumulation in the symbiotic protocorm suggests that *T. calospora* is experiencing an oxidative environment and responds with the accumulation of antioxidants.

Chitin and chitin-derived metabolites in symbiosis

Chitin is the main structural component of the fungal cell wall (Bowman & Free, 2006) and contains nitrogen in the form of N-acetyl glucosamine residues, joined by beta-(1,4) linkages. In addition to a structural role, chitin is a source of signaling molecules that regulate plant-microbe interactions (Sánchez-Vallet *et al.*, 2015). Chito-oligosaccharides with a degree of

polymerization of 6 to 8 act as signal molecules and are strong inducers of plant defense responses against pathogenic fungi because they are recognized by chitin-specific plant receptors (Pusztahelyi, 2018). The chitin oligomers accumulated in symbiotic *S. vomeracea* protocorms, as compared with MYC and FLM samples, were much smaller, with a degree of polymerization of 3 (chitotriose, $\log_2=13.6$) and 2 (chitobiose, $\log_2=11.9$). Chitin oligomers may originate by either a biosynthetic process or cleavage of a longer chitin polymer. Bacterial and fungal plant mutualists can synthesize chitin-derived signaling molecules to prepare their hosts for colonization (Sánchez-Vallet *et al.*, 2015). Alternatively, chito-oligosaccharides can be released from chitin by fungal and plant chitinases. Plant chitinases are involved in defense against fungal pathogens because they hydrolyze fungal cell wall chitinous components and release chitin oligomers that trigger the plant immune responses (Fukamizo & Shinya, 2019). Most plant chitinases are endochitinases that cleave randomly at internal sites in the chitin polymer, generating low molecular mass glucosamine multimers (Rathore & Gupta, 2015). Although we do not have direct evidence of the origin of the chitotriose and chitobiose compounds in *S. vomeracea* symbiotic protocorms, transcriptomic data support the hypothesis that they are generated by the activity of plant chitinases. In fact, only one of the two *T. calospora* chitin synthase genes expressed in symbiotic protocorms was slightly upregulated (FC=2, Table S2). Conversely, transcripts corresponding to plant chitinases belonging to GH18 and GH19 families were strongly upregulated in symbiotic protocorms (Table S3), in agreement with previous observations showing increased chitinase expression in symbiotic protocorms (Zhao *et al.*, 2013; Perotto *et al.*, 2014). Although plants produce endochitinases in response to phytopathogenic attacks (Kumar *et al.*, 2018), a role for chitinases in root symbioses has already been reported for AM and nodule symbioses. In AM roots, the strong expression of chitinases in arbusculated cells, mainly belonging to class III (GH family 18), is thought to reduce the amount of chitin elicitors released by the wall of a compatible symbiotic fungus (Kasprzewska, 2003; Hoge-kamp *et al.*, 2011; Grover, 2012). Interestingly, short oligomers of 2 to 5 N-acetyl glucosamine residues, similar to those found in this work, have been reported to actively promote AM colonization (Volpe *et al.*, 2020). Further studies are required to elucidate the involvement of *S. vomeracea* chitinases during the OM symbiosis.

Chitosan oligomers were also abundant in the SYMB samples. Chitosan is the deacetylated form of chitin and is not abundant in the cell wall of Basidiomycetes (Di Mario *et al.* 2008). It was therefore intriguing to find a similar enrichment of chitin and chitosan oligomers (\log_2 from 12.0 to 13.5) in symbiotic protocorms (Table S1), when compared with either the MYC

or the FLM samples. Chitosan is produced through the activity of chitin deacetylase and three *T. calospora* chitin deacetylase genes were significantly upregulated in the symbiotic protocorms, as compared with FLM (Table S2), supporting the hypothesis that chitin deacetylation is increased in symbiosis. Chitin deacetylase inactivates the elicitor activity of chitin oligomers because it converts them to ligand-inactive chitosan. Chitin deacetylation has been reported as a strategy of endophytic fungi and soil-borne pathogens to prevent chitin-triggered plant immunity (Cord-Landwehr *et al.*, 2016; Gao *et al.*, 2019). Also, chitin deacetylases are regulated during the interaction with plants in both ECM and AM fungi (Balestrini & Bonfante, 2014), suggesting a role during symbiosis establishment and functioning.

Current challenges of metabolomic studies of poorly described organisms

Metabolomics is a powerful tool to investigate biological systems. Here, it provided a global profiling of the metabolites and it allowed the study of orchid mycorrhiza. We demonstrated a rearrangement of the metabolome and changes in compounds possibly related to structural, signaling, defense, and nutrient functions.

However, the metabolomic approach also showed some limitations. For example, several mass-features could not be annotated in the available database. This uncharacterized “dark matter” is surely an interesting chemical signature that contains crucial information. For instance, from the 291 and 315 mass-features uniquely found in MYC-SYMB or in MYC-SYMB-FLM (Fig. 2), respectively representing symbiosis-specific and constitutive fungal compounds, none could be reasonably matched in databases. Overall, there is still a severe limitation in metabolite annotation in non-targeted metabolomics study: only ~2% of spectra is currently found in databases (da Silva *et al.*, 2015). This is much less than for genomic studies, where annotation can reach ~80%. Further difficulties of metabolomic studies arise from the fact that metabolomics reports are usually focused on model organisms, hampering functional enrichment analysis of non-model organisms such as *T. calospora* and *S. vomeracea*. Orchids and the symbiotic fungus *T. calospora* are evolutionary distant to those organisms found in the database and, in the case of orchids, rich of yet unknown secondary metabolites (Sut *et al.*, 2017). For the current study, we used MetaCyc, the largest curated collection of metabolic pathways, and the most comprehensive reference database of metabolic pathways from all domains of life (Caspi *et al.*, 2018). It contains the experimental evidence of 457 pathways in a member of the taxonomic group fungi, from >54,000 publications (Caspi *et al.*, 2019; Karp *et al.*, 2019). However, even when using such extensive

collection, 451 metabolites in the comparison MYC/FLM could not be matched to objects in the database, pointing to the abovementioned limitation in the reconstruction of the biochemical pathways of *S. vomeracea* and *T. calospora*. Nevertheless, despite the severe limitations in metabolite annotation and functional analysis, we could estimate the elemental formulas of detected mass features. Using an ultra-high mass resolution and following the “seven golden rules” (Kind & Fiehn, 2007), we could accurately measure the mass-to-charge ratios of the metabolome fingerprint and produce an excellent estimation of the metabolite elemental formula with a high probability (Kim *et al.*, 2006, probability of 98%). Atom ratios of compound elemental formulas can be visualized using van Krevelen diagrams for rough compound identification in chemical classes, although the limits defining those classes are overlapping among the compound categories. To overcome this issue, we employed the very recently developed multidimensional stoichiometric compound classification (MSCC) approach (Rivas-Ubach *et al.*, 2018). In this way, we successfully classified almost entirely the significant mass-features discriminant for the separation of MYC/FLM, MYC/SYMB, SYMB/ASYMB and overcame constraints of actual database.

In conclusion, we revealed profound changes in metabolite profiles in orchid mycorrhiza. The most interesting finding was the sharp adjustment of the lipid metabolism in the fungus *T. calospora* to the symbiosis. Although further and more sensitive targeted analyses are needed to elucidate the significance of these metabolic changes in symbiosis, our study demonstrates that the cross-link between metabolomic and transcriptomic data can pave the way for a more comprehensive understanding of the metabolic networks underlying orchid-fungus interactions.

ACKNOWLEDGMENTS

The orchid mycorrhizal genome and transcriptomes were sequenced at the US Department of Energy Joint Genome Institute within the framework of the Mycorrhizal Genomics Initiative (CSP#305, Exploring the Genome Diversity of Mycorrhizal Fungi to Understand the Evolution and Functioning of Symbiosis in Woody Shrubs and Trees) coordinated by Francis Martin (INRA, Nancy, France).

AUTHOR CONTRIBUTIONS

S.P., R.B. and J.P.S. conceived and designed the research. A.G., V.F. and B.L. conducted all wet lab experiments. A.G., J.P.S. and M.W. conducted data analyses. A.G., S.P., R.B. wrote the manuscript. All authors read and approved the manuscript.

REFERENCES

- Aharoni A, Ric de Vos CH, Verhoeven HA, Maliepaard CA, Kruppa G, Bino R, Goodenowe DB. 2002.** Nontargeted metabolome analysis by use of Fourier Transform Ion Cyclotron Mass Spectrometry. *OMICS A Journal of Integrative Biology* **6**: 217–234.
- Balestrini R, Bonfante P. 2014.** Cell wall remodeling in mycorrhizal symbiosis: A way towards biotrophism. *Frontiers in Plant Science* **5**: 1–10.
- Balla T. 2013.** Phosphoinositides: Tiny lipids with giant impact on cell regulation. *Physiological Reviews* **93**: 1019–1137.
- Beyrle HF, Smith SE, Peterson RL, Franco CM. 1995.** Colonization of *Orchis morio* protocorms by a mycorrhizal fungus: Effects of nitrogen nutrition and glyphosate in modifying the responses. *Canadian Journal of Botany* **73**: 1128–1140.
- Blunsom NJ, Cockcroft S. 2020.** Phosphatidylinositol synthesis at the endoplasmic reticulum. *Biochimica et Biophysica Acta - Molecular and Cell Biology of Lipids* **1865**: 158471.
- Bowers WS, Hoch HC, Evans PH, Katayama M. 1986.** Thallophtic allelopathy: Isolation and identification of laetisarinic acid. *Science* **232**: 105–106.
- Bowman SM, Free SJ. 2006.** The structure and synthesis of the fungal cell wall. *BioEssays* **28**: 799–808.
- Brodhun F, Feussner I. 2011.** Oxylipins in fungi. *FEBS Journal* **278**: 1047–1063.
- Cameron DD, Johnson I, Leake JR, Read DJ. 2007.** Mycorrhizal acquisition of inorganic phosphorus by the green-leaved terrestrial orchid *Goodyera repens*. *Annals of Botany* **99**: 831–834.
- Cameron DD, Johnson I, Read DJ, Leake JR. 2008.** Giving and receiving: Measuring the carbon cost of mycorrhizas in the green orchid, *Goodyera repens*. *New Phytologist* **180**: 176–184.
- Cameron DD, Leake JR, Read DJ. 2006.** Mutualistic mycorrhiza in orchids: Evidence from plant-fungus carbon and nitrogen transfers in the green-leaved terrestrial orchid *Goodyera*

660 *repens*. *New Phytologist* **171**: 405–416.

661 **Carta G, Murru E, Banni S, Manca C. 2017.** Palmitic acid: Physiological role, metabolism
662 and nutritional implications. *Frontiers in Physiology* **8**: 1–14.

663 **Caspi R, Billington R, Fulcher CA, Keseler IM, Kothari A, Krummenacker M,**
664 **Latendresse M, Midford PE, Ong Q, Ong WK, et al. 2018.** The MetaCyc database of
665 metabolic pathways and enzymes. *Nucleic Acids Research* **46**: D633–D639.

666 **Caspi R, Billington R, Keseler IM, Kothari A, Krummenacker M, Midford PE, Ong**
667 **WK, Paley S, Subhraveti P, Karp PD. 2019.** The MetaCyc database of metabolic pathways
668 and enzymes - a 2019 update. *Nucleic Acids Research* **1**: 1–9.

669 **Cassilly CD, Reynolds TB. 2018.** PS, it's complicated: The roles of phosphatidylserine and
670 phosphatidylethanolamine in the pathogenesis of *Candida albicans* and other microbial
671 pathogens. *Journal of Fungi* **4**: 28.

672 **Cavill R, Jennen D, Kleinjans J, Briedé JJ. 2016.** Transcriptomic and metabolomic data
673 integration. *Briefings in Bioinformatics* **17**: 891–901.

674 **Chang DCN, Chou LC. 2007.** Growth responses, enzyme activities, and component changes
675 as influenced by *Rhizoctonia* Orchid mycorrhiza on *Anoectochilus formosanus* Hayata.
676 *Botanical Studies* **48**: 445–451.

677 **Christensen SA, Kolomiets M V. 2011.** The lipid language of plant-fungal interactions.
678 *Fungal Genetics and Biology* **48**: 4–14.

679 **Cord-Landwehr S, Melcher RLJ, Kolkenbrock S, Moerschbacher BM. 2016.** A chitin
680 deacetylase from the endophytic fungus *Pestalotiopsis* sp. efficiently inactivates the elicitor
681 activity of chitin oligomers in rice cells. *Scientific Reports* **6**: 1–11.

682 **Cowan AK. 2006.** Phospholipids as plant growth regulators. *Plant Growth Regulation* **48**:
683 97–109.

684 **Cumming BM, Chinta KC, Reddy VP, Steyn AJC. 2018.** Role of Ergothioneine in
685 Microbial Physiology and Pathogenesis. *Antioxidants and Redox Signaling* **28**: 431–444.

686 **Dearnaley JDW, Cameron DD. 2017.** Nitrogen transport in the orchid mycorrhizal
687 symbiosis – further evidence for a mutualistic association. *New Phytologist* **213**: 10–12.

688 **Ebert B, Rautengarten C, McFarlane HE, Rupasinghe T, Zeng W, Ford K, Scheller H**
689 **V., Bacic A, Roessner U, Persson S, et al. 2018.** A Golgi UDP-GlcNAc transporter delivers
690 substrates for N-linked glycans and sphingolipids. *Nature Plants* **4**: 792–801.

691 **Epstein S, Castillon GA, Qin Y, Riezman H. 2012.** An essential function of sphingolipids in
692 yeast cell division. *Molecular Microbiology* **84**: 1018–1032.

693 **Ercole E, Adamo M, Rodda M, Gebauer G, Girlanda M, Perotto S. 2015a.** Temporal

variation in mycorrhizal diversity and carbon and nitrogen stable isotope abundance in the wintergreen meadow orchid *Anacamptis morio*. *New Phytologist* **205**: 1308–1319.

Ercole E, Rodda M, Girlanda M, Perotto S. 2015b. Establishment of a symbiotic in vitro system between a green meadow orchid and a Rhizoctonia-like fungus. *Bio-protocol* **5**: 1–7.

Fiehn O, Kopka J, Dörmann P, Altmann T, Trethewey RN, Willmitzer L. 2000. Metabolite profiling for plant functional genomics. *Nature Biotechnology* **18**: 1157–1161.

Fochi V, Chitarra W, Kohler A, Voyron S, Singan VR, Lindquist EA, Barry KW, Girlanda M, Grigoriev I V., Martin F, et al. 2017a. Fungal and plant gene expression in the *Tulasnella calospora* – *Serapias vomeracea* symbiosis provides clues about nitrogen pathways in orchid mycorrhizas. *New Phytologist* **213**: 365–379.

Fochi V, Falla N, Girlanda M, Perotto S, Balestrini R. 2017b. Cell-specific expression of plant nutrient transporter genes in orchid mycorrhizae. *Plant Science* **263**: 39–45.

Fukamizo T, Shinya S. 2019. Chitin/Chitosan-Active Enzymes Involved in Plant–Microbe Interactions. In: Yang Q, Fukamizo T, eds. *Targeting Chitin-containing Organisms. Advances in Experimental Medicine and Biology*. Singapore: Springer, Vol. 1142, 253–272.

Furo K, Nozaki M, Murashige H, Sato Y. 2015. Identification of an *N*-acetylglucosamine kinase essential for UDP-*N*-acetylglucosamine salvage synthesis in *Arabidopsis*. *FEBS Letters* **589**: 3258–3262.

Fyrst H, Saba JD. 2010. An update on sphingosine-1-phosphate and other sphingolipid mediators. *Nature Chemical Biology* **6**: 489–497.

Gao F, Zhang B Sen, Zhao JH, Huang JF, Jia PS, Wang S, Zhang J, Zhou JM, Guo HS. 2019. Deacetylation of chitin oligomers increases virulence in soil-borne fungal pathogens. *Nature Plants* **5**: 1167–1176.

Gerke J, Bayram Ö, Braus GH. 2012. Fungal S-adenosylmethionine synthetase and the control of development and secondary metabolism in *Aspergillus nidulans*. *Fungal Genetics and Biology* **49**: 443–454.

Ghirardo A, Heller W, Fladung M, Schnitzler J-P, Schroeder H. 2012. Function of defensive volatiles in pedunculate oak (*Quercus robur*) is tricked by the moth *Tortrix viridana*. *Plant, Cell and Environment environment* **35**: 2192–2207.

Ghirardo A, Sørensen HA, Petersen M, Jacobsen S, Søndergaard I. 2005. Early prediction of wheat quality: analysis during grain development using mass spectrometry and multivariate data analysis. *Rapid communications in mass spectrometry* **19**: 525–532.

Ghirardo A, Xie J, Zheng X, Wang Y, Grote R, Block K, Wildt J, Mentel T, Kiendler-Scharr A, Hallquist M, et al. 2016. Urban stress-induced biogenic VOC emissions impact

secondary aerosol formation in Beijing. *Atmospheric Chemistry and Physics* **15**: 2901–2920.

Girlanda M, Segreto R, Cafasso D, Liebel HT, Rodda M, Ercole E, Cozzolino S, Gebauer G, Perotto S. 2011. Photosynthetic Mediterranean meadow orchids feature partial mycoheterotrophy and specific mycorrhizal associations¹. *American Journal of Botany* **98**: 1148–1163.

Grover A. 2012. Plant Chitinases: Genetic Diversity and Physiological Roles. *Critical Reviews in Plant Sciences* **31**: 57–73.

Hannun YA, Obeid LM. 2018. Sphingolipids and their metabolism in physiology and disease. *Nature Reviews Molecular Cell Biology* **19**: 175–191.

Hogekamp C, Arndt D, Pereira PA, Becker JD, Hohnjec N, Küster H. 2011. Laser microdissection unravels cell-type-specific transcription in arbuscular mycorrhizal roots, including CAAT-Box transcription factor gene expression correlating with fungal contact and spread. *Plant Physiology* **157**: 2023–2043.

Hou Q, Ufer G, Bartels D. 2016. Lipid signalling in plant responses to abiotic stress. *Plant Cell and Environment* **39**: 1029–1048.

Hu W, Pan X, Abbas HMK, Li F, Dong W. 2017. Metabolites contributing to *Rhizoctonia solani* AG-1-IA maturation and sclerotial differentiation revealed by UPLC-QTOF-MS metabolomics. *PLoS ONE* **12**: 1–16.

Kaling M, Kanawati B, Ghirardo A, Albert A, Winkler JB, Heller W, Barta C, Loreto F, Schmitt-Kopplin P, Schnitzler J-PP. 2015. UV-B mediated metabolic rearrangements in poplar revealed by non-targeted metabolomics. *Plant, cell & environment* **38**: 892–904.

Kårlund A, Hanhineva K, Lehtonen M, Karjalainen RO, Sandell M. 2015. Nontargeted metabolite profiles and sensory properties of strawberry cultivars grown both organically and conventionally. *Journal of Agricultural and Food Chemistry* **63**: 1010–1019.

Karp PD, Billington R, Caspi R, Fulcher CA, Latendresse M, Kothari A, Keseler IM, Krummenacker M, Midford PE, Ong Q, et al. 2019. The BioCyc collection of microbial genomes and metabolic pathways. *Briefings in Bioinformatics* **20**: 1085–1093.

Kasprzewska A. 2003. Plant chitinases - Regulation and function. *Cellular and Molecular Biology Letters* **8**: 809–824.

Kay JG, Grinstein S. 2011. Sensing phosphatidylserine in cellular membranes. *Sensors* **11**: 1744–1755.

Kersten B, Ghirardo A, Schnitzler J, Kanawati B, Schmitt-Kopplin P, Fladung M, Schroeder H. 2013. Integrated transcriptomics and metabolomics decipher differences in the resistance of pedunculate oak to the herbivore *Tortrix viridana* L. *BMC genomics* **14**: 737.

Keymer A, Pimprikar P, Wewer V, Huber C, Brands M, Bucerius SL, Delaux P, Klingl V, Wang TL, Eisenreich W. 2017. Lipid transfer from plants to arbuscular mycorrhiza fungi. *6:e29107*.

Kim S, Rodgers RP, Marshall AG. 2006. Truly ‘exact’ mass: Elemental composition can be determined uniquely from molecular mass measurement at ~0.1 mDa accuracy for molecules up to ~500 Da. *International Journal of Mass Spectrometry* **251**: 260–265.

Kind T, Fiehn O. 2007. Seven Golden Rules for heuristic filtering of molecular formulas obtained by accurate mass spectrometry. *BMC Bioinformatics* **8**: 1–20.

Kluger B, Lehner S, Schuhmacher R. 2015. Metabolomics and secondary metabolite profiling of filamentous fungi. In: Zeilinger S, Martín J, García-Estrada C, eds. *Biosynthesis and Molecular Genetics of Fungal Secondary Metabolites Volume 2. Fungal Biology*. New York: Springer, 81–101.

Kohler A, Böcker U, Shapaval V, Forsmark A, Andersson M, Warringer J, Martens H, Omholt SW, Blomberg A. 2015a. High-throughput biochemical fingerprinting of *Saccharomyces cerevisiae* by Fourier transform infrared spectroscopy. *PLoS ONE* **10**: 1–22.

Kohler A, Kuo A, Nagy LG, Morin E, Barry KW, Buscot F, Canbäck B, Choi C, Cichocki N, Clum A, et al. 2015b. Convergent losses of decay mechanisms and rapid turnover of symbiosis genes in mycorrhizal mutualists. *Nature Genetics* **47**: 410–415.

Kuga Y, Sakamoto N, Yurimoto H. 2014. Stable isotope cellular imaging reveals that both live and degenerating fungal pelotons transfer carbon and nitrogen to orchid protocorms. *New Phytologist* **202**: 594–605.

Kumar M, Brar A, Yadav M, Chawade A, Vivekanand V, Pareek N. 2018. Chitinases—Potential candidates for enhanced plant resistance towards fungal pathogens. *Agriculture* **8**.

Lallemand F, Martin-Magniette ML, Gilard F, Gakière B, Launay-Avon A, Delannoy É, Selosse MA. 2019. *In situ* transcriptomic and metabolomic study of the loss of photosynthesis in the leaves of mixotrophic plants exploiting fungi. *Plant Journal* **98**: 826–841.

Laparre J, Malbreil M, Letisse F, Portais JC, Roux C, Bécard G, Puech-Pagès V. 2014. Combining metabolomics and gene expression analysis reveals that propionyl- and butyryl-carnitines are involved in late stages of arbuscular mycorrhizal symbiosis. *Molecular Plant* **7**: 554–566.

Leake JR. 1994. Tansley Review No. 69. The biology of myco-heterotrophic ('saprophytic') plants. *New Phytol.* **127**: 171–216.

Liu X-H, Liang S, Wei Y-Y, Zhu X-M, Li L, Ping-Ping Liu B, Zheng Q-X, Zhou H-N, Zhang Y, Mao L-J, et al. 2019. Metabolomics Analysis Identifies Sphingolipids as Key

796 Function in *Magnaporthe oryzae*. *American Society For Microbiology* **10**: 1–18.

797 **Majumder PL, Lahiri S. 1990.** Lusianthrin and lusianthridin, two stilbenoids from the
798 orchid *Lusia indivisa*. *Phytochemistry* **29**: 621–624.

799 **Di Mario F, Rapanà P, Tomati U, Galli E. 2008.** Chitin and chitosan from Basidiomycetes.
800 *International Journal of Biological Macromolecules* **43**: 8–12.

801 **Mato JM, Alvarez L, Ortiz P, Pajares MA. 1997.** S-adenosylmethionine synthesis:
802 Molecular mechanisms and clinical implications. *Pharmacology and Therapeutics* **73**: 265–
803 280.

804 **Meijer HJG, Munnik T. 2003.** Phospholipid-Based Signaling in Plants. *Annual Review of*
805 *Plant Biology* **54**: 265–306.

806 **Michell RH. 2008.** Inositol derivatives: Evolution and functions. *Nature Reviews Molecular*
807 *Cell Biology* **9**: 151–161.

808 **Miura C, Yamaguchi K, Miyahara R, Yamamoto T, Fuji M, Yagame T, Imaizumi-**
809 **Anraku H, Yamato M, Shigenobu S, Kaminaka H. 2018.** The mycoheterotrophic
810 symbiosis between orchids and mycorrhizal fungi possesses major components shared with
811 mutualistic plant-mycorrhizal symbioses. *Molecular Plant-Microbe Interactions* **31**: 1032–
812 1047.

813 **Obeid LM, Okamoto Y, Mao C. 2002.** Yeast sphingolipids: Metabolism and biology.
814 *Biochimica et Biophysica Acta - Molecular and Cell Biology of Lipids* **1585**: 163–171.

815 **Oura T, Kajiwara S. 2010.** *Candida albicans* sphingolipid C9-methyltransferase is involved
816 in hyphal elongation. *Microbiology* **156**: 1234–1243.

817 **Paley S, Parker K, Spaulding A, Tomb JF, O’Maille P, Karp PD. 2017.** The omics
818 dashboard for interactive exploration of gene-expression data. *Nucleic Acids Research* **45**:
819 12113–12124.

820 **Pegg AE, Xiong H, Feith DJ, Shantz LM. 1998.** S-adenosylmethionine decarboxylase:
821 Structure, function and regulation by polyamines. *Biochemical Society Transactions* **26**: 580–
822 586.

823 **Perotto S, Rodda M, Benetti A, Sillo F, Ercole E, Rodda M, Girlanda M, Murat C,**
824 **Balestrini R. 2014.** Gene expression in mycorrhizal orchid protocorms suggests a friendly
825 plant-fungus relationship. *Planta* **239**: 1337–1349.

826 **Peterson RL, Farquhar ML. 1994.** Mycorrhizas: Integrated development between roots and
827 fungi. *Mycologia* **86**: 311–326.

828 **Plassard C, Becquer A, Garcia K. 2019.** Phosphorus Transport in Mycorrhiza: How Far Are
829 We? *Trends in Plant Science* **24**: 794–801.

830 **Pusztahelyi T. 2018.** Chitin and chitin-related compounds in plant–fungal interactions.
831 *Mycology* **9**: 189–201.

832 **Rasmussen HN. 1995.** *Terrestrial orchids: from seed to mycotrophic plant* (Cambridge, Ed.).
833 Cambridge, UK: Cambridge University Press.

834 **Rathore AS, Gupta RD. 2015.** Chitinases from bacteria to human: properties, applications,
835 and future perspectives. *Enzyme Research* **2015**: 1–9.

836 **Rivas-Ubach A, Liu Y, Bianchi TS, Tolić N, Jansson C, Paša-Tolić L. 2018.** Moving
837 beyond the van Krevelen diagram: A new stoichiometric approach for compound
838 classification in organisms. *Analytical Chemistry* **90**: 6152–6160.

839 **Rivero J, Gamir J, Aroca R, Pozo MJ, Flors V. 2015.** Metabolic transition in mycorrhizal
840 tomato roots. *Frontiers in Microbiology* **6**: 598.

841 **Sánchez-Vallet A, Mesters JR, Thomma BPHJ. 2015.** The battle for chitin recognition in
842 plant-microbe interactions. *FEMS Microbiology Reviews* **39**: 171–183.

843 **Schliemann W, Ammer C, Strack D. 2008.** Metabolite profiling of mycorrhizal roots of
844 *Medicago truncatula*. *Phytochemistry* **69**: 112–146.

845 **Schumann U, Smith NA, Wang MB. 2013.** A fast and efficient method for preparation of
846 high-quality RNA from fungal mycelia. *BMC Research Notes* **6**: 71.

847 **Sheridan KJ, Lechner BE, Keeffe GO, Keller MA, Werner ER, Lindner H, Jones GW,
848 Haas H, Doyle S. 2016.** Ergothioneine biosynthesis and functionality in the opportunistic
849 fungal pathogen, *Aspergillus fumigatus*. *Scientific Reports* **6**: 1–17.

850 **Shimura H, Matsuura M, Takada N, Koda Y. 2007.** An antifungal compound involved in
851 symbiotic germination of *Cypripedium macranthos* var. *rebunense* (Orchidaceae).
852 *Phytochemistry* **68**: 1442–1447.

853 **Sidorov RA, Zhukov A V., Pchelkin VP, Tsydendambaev VD. 2014.** Palmitic acid in
854 higher plant lipids. In: *Palmitic Acid: Occurrence, Biochemistry and Health Effects*. Nova
855 Science Publishers, Inc., 124–144.

856 **Siebers M, Brands M, Wewer V, Duan Y, Hölzl G, Dörmann P. 2016.** Lipids in plant–
857 microbe interactions. *Biochimica et Biophysica Acta - Molecular and Cell Biology of Lipids*
858 **1861**: 1379–1395.

859 **da Silva RR, Dorrestein PC, Quinn RA. 2015.** Illuminating the dark matter in
860 metabolomics. *Proceedings of the National Academy of Sciences of the United States of*
861 *America* **112**: 12549–12550.

862 **Singh A, Del Poeta M. 2016.** Sphingolipidomics: An important mechanistic tool for studying
863 fungal pathogens. *Frontiers in Microbiology* **7**: 1–14.

864 **Smith S, Read D. 2008.** *Mycorrhizal symbiosis*. Cambridge, UK: Academic Press.

865 **Suhre K, Schmitt-Kopplin P. 2008.** MassTRIX: mass translator into pathways. *Nucleic*

866 *acids research* **36**: 481–484.

867 **Sut S, Maggi F, Dall’Acqua S. 2017.** Bioactive Secondary Metabolites from Orchids

868 (Orchidaceae). *Chemistry and Biodiversity* **14**: e1700172.

869 **Tschapinski TJ, Plett JM, Engle NL, Deveau A, Cushman KC, Martin MZ, Doktycz**

870 **MJ, Tuskan GA, Brun A, Kohler A, et al. 2014.** *Populus trichocarpa* and *Populus deltoides*

871 Exhibit Different Metabolomic Responses to Colonization by the Symbiotic Fungus *Laccaria*

872 *bicolor*. *Molecular Plant-Microbe Interactions* **27**: 546–556.

873 **Valentín-Berríos S, González-Velázquez W, Pérez-Sánchez L, González-Méndez R,**

874 **Rodríguez-Del Valle N. 2009.** Cytosolic phospholipase A: a member of the signalling

875 pathway of a new G protein α subunit in *Sporothrix schenckii*. *BMC Microbiology* **9**: 1–16.

876 **Vences-Guzmán MA, Geiger O, Sohlenkamp C. 2008.** Sinorhizobium meliloti mutants

877 deficient in phosphatidylserine decarboxylase accumulate phosphatidylserine and are strongly

878 affected during symbiosis with alfalfa. *Journal of Bacteriology* **190**: 6846–6856.

879 **Volpe V, Carotenuto G, Berzero C, Cagnina L, Puech-Pagès V, Genre A. 2020.** Short

880 chain chito-oligosaccharides promote arbuscular mycorrhizal colonization in *Medicago*

881 *truncatula*. *Carbohydrate Polymers* **229**: 115505.

882 **Van Waes JM, Debergh PC. 1986.** In vitro germination of some Western European orchids.

883 *Physiologia Plantarum* **67**: 253–261.

884 **Wägele B, Witting M, Schmitt-Kopplin P, Suhre K. 2012.** Masstrix reloaded: Combined

885 analysis and visualization of tran-scriptome and metabolome data. *PLoS ONE* **7**: 1–5.

886 **Wang K Der, Borrego EJ, Kenerley CM, Kolomiets M V. 2020.** Oxylipins Other Than

887 Jasmonic Acid Are Xylem-Resident Signals Regulating Systemic Resistance Induced by

888 *Trichoderma virens* in Maize. *The Plant cell* **32**: 166–185.

889 **Way D, Ghirardo A, Kanawati B, Esperschütz J, Monson RK, Jackson RB, Schmitt-**

890 **Kopplin P, Schnitzler J-P. 2013.** Increasing atmospheric CO₂ reduces metabolic and

891 physiological differences between isoprene- and non-isoprene-emitting poplars. *The New*

892 *phytologist* **200**: 534–546.

893 **Yeh CM, Chung KM, Liang CK, Tsai WC. 2019.** New insights into the symbiotic

894 relationship between orchids and fungi. *Applied Sciences* **9**: 1–14.

895 **Zhang N, Venkateshwaran M, Boersma M, Harms A, Howes-Podoll M, Den Os D, Ané**

896 **JM, Sussman MR. 2012.** Metabolomic profiling reveals suppression of oxylipin biosynthesis

897 during the early stages of legume-rhizobia symbiosis. *FEBS Letters* **586**: 3150–3158.

898 **Zhao MM, Zhang G, Zhang DW, Hsiao YY, Guo SX. 2013.** ESTs analysis reveals putative
899 genes involved in symbiotic seed germination in *Dendrobium officinale*. *PLoS ONE* **8**:
900 e72705.
901
902

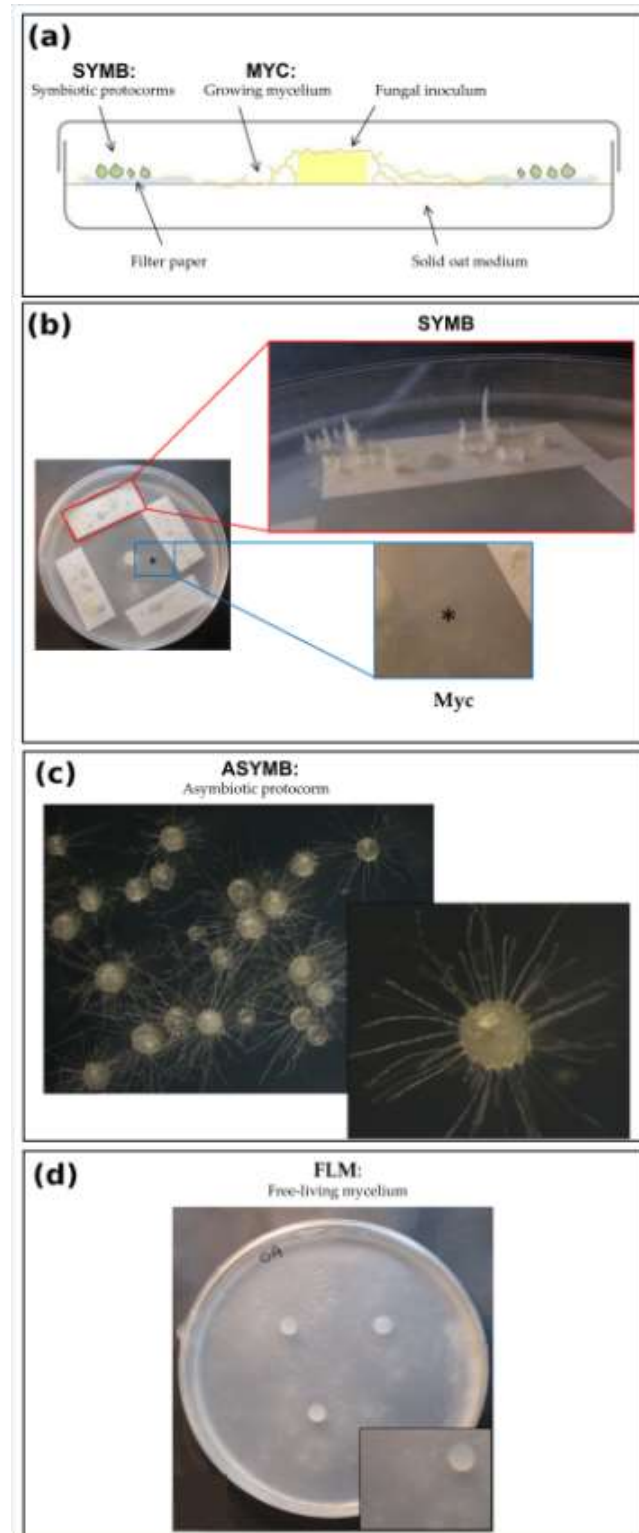
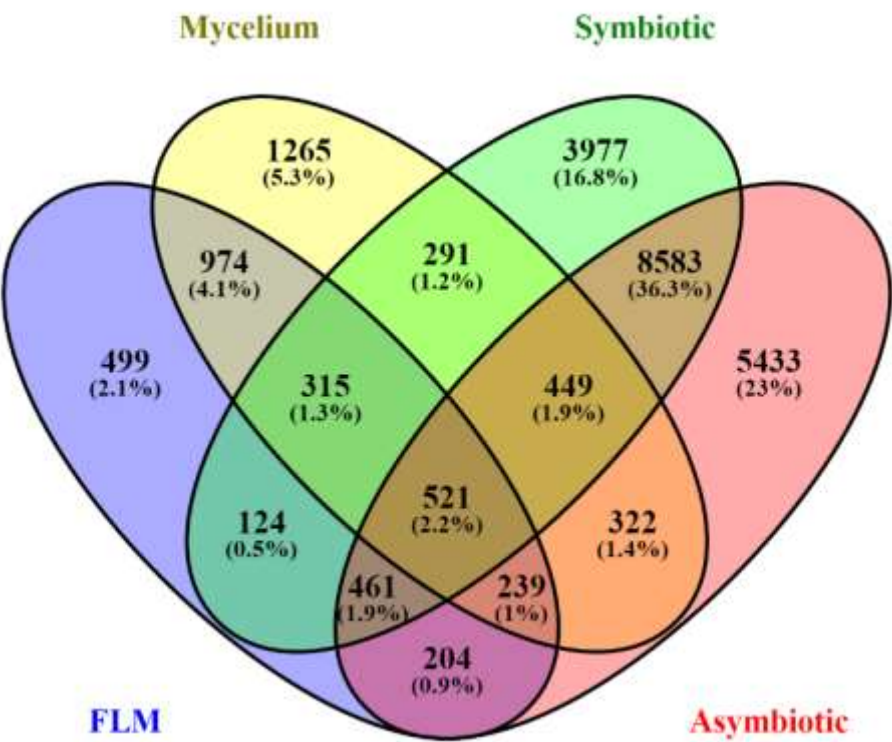


Figure 1: (a) Schematic representation of the *in vitro* symbiotic germination system of *Serapias vomeracea* seeds with the orchid mycorrhizal fungus *Tulasnella calospora* (redraw from (Ercole *et al.*, 2015b)). (b) Symbiotic seed germination in Petri dishes; Mycorrhizal symbiotic protocorms (SYMB) of *S. vomeracea* (red box) and fungal mycelium (MYC) growing near the symbiotic protocorms (blue box) after 30 days of co-incubation. (c) Asymbiotic protocorms (ASYMB) grown on BM1 medium 120 days after sowing. (d) Free-living mycelium (FLM) of *T. calospora* grown on oat medium (OA) at 20 dpi.



914

915

916

917

918

919

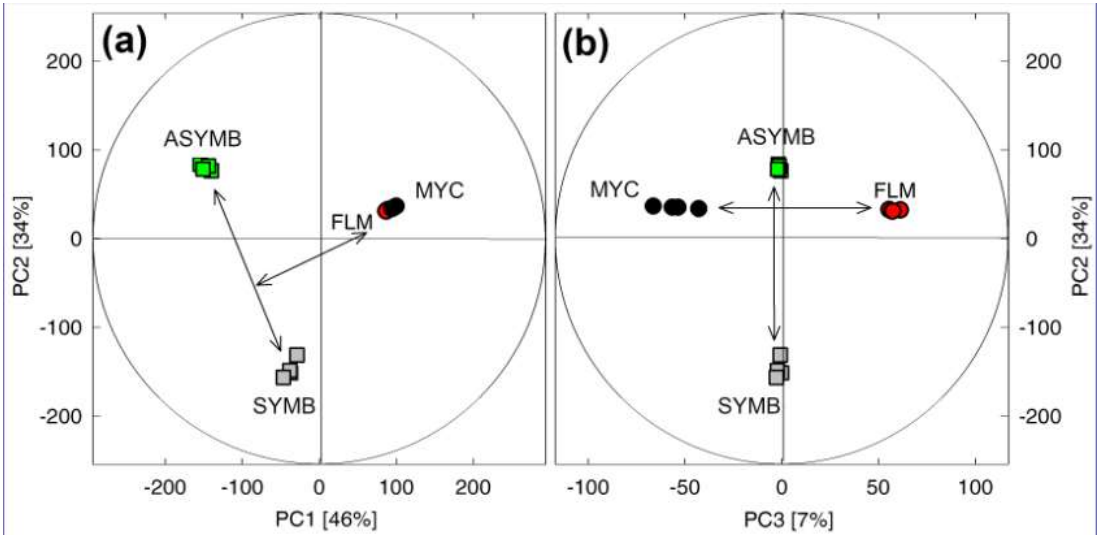
920

921

922

Figure 2: Venn diagram of specific and shared mass features (m.f.) occurring and overlapping in symbiotic (SYMB) and asymbiotic (ASYMB) *S. vomeracea* protocorms, *T. calospora* free-living mycelium (FLM) and mycelium growing near symbiotic protocorms (MYC).

923



924

925

926

927

928

929

930

931

932

933

934

935

936

Figure 3: Score plots of principal components analysis (PCA) of all mass features detected by non-targeted metabolomics. **(a)** Principal component (PC) 1 vs. PC2 shows the metabolic distances between *T. calospora* AL13 growing as free-living mycelium (FLM) or collected near the symbiotic protocorms (MYC) and between *S. vomeracea* symbiotic (SYMB) and asymbiotic (ASYMB) protocorms. **(b)** PC3 depicts metabolic differences between MYC and FLM. The variances explained by each PC are given in parentheses. Ellipses denote the Hotelling's T^2 confidence interval of 95%. N = 4 biologically independent replicates. FLM, red circles; MYC, black circles; ASYMB, green square; SYMB, grey square.

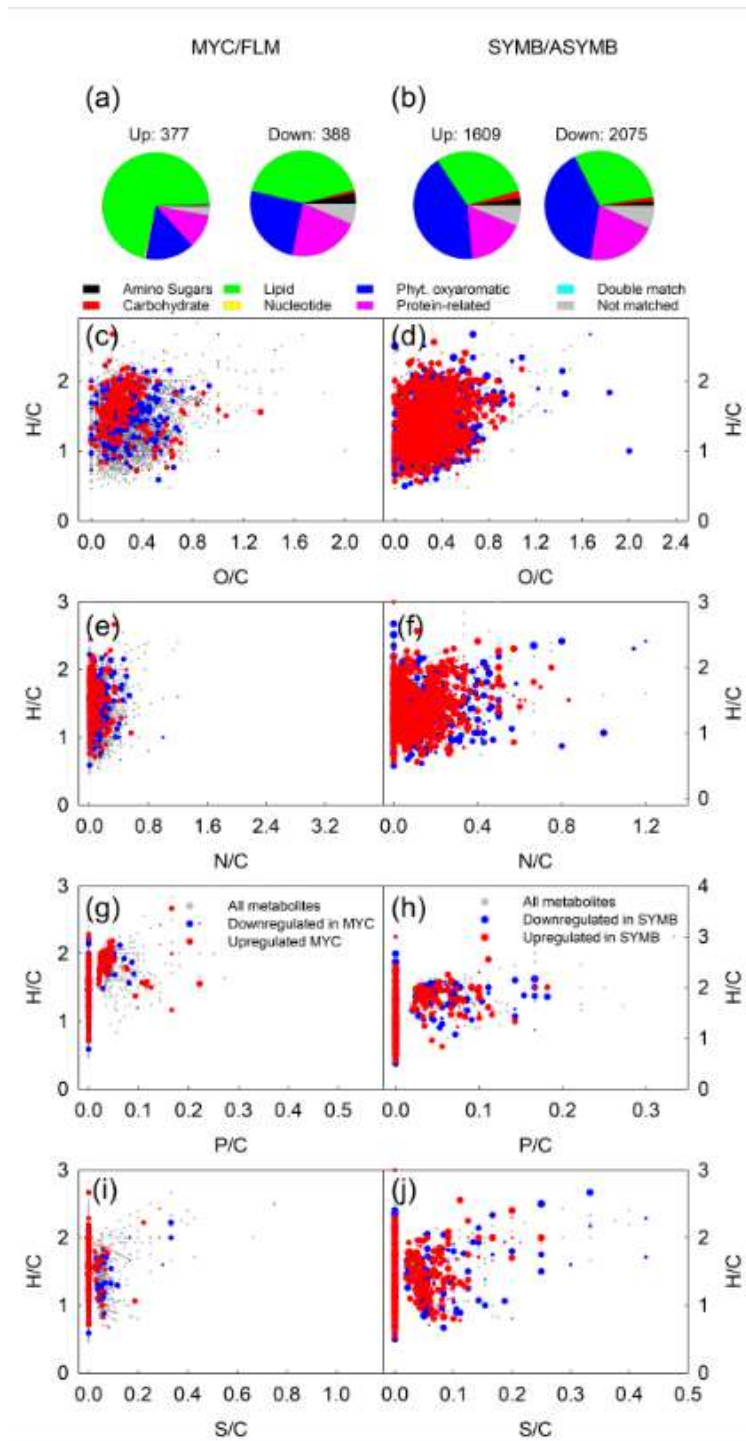


Figure 4: (a-b), Multidimensional stoichiometric compound classification (MSCC), and van Krevelen diagrams (c-j) showing all metabolites (in grey) and statistically up- (in red) or down- (in blue) regulated metabolites in asymbiotic and symbiotic conditions. Abbr. MYC, fungal mycelium growing near the mycorrhizal protocorms; FLM, asymbiotic free-living mycelium; SYMB, symbiotic orchid protocorms; ASYMB, asymbiotic orchid protocorms. The magnitude of up- and down-regulated metabolites are depicted in (c-j) with different symbol sizes (larger symbols represent stronger up/downregulation), using $\sqrt{(\log_2(x))/2}$ for upregulated and $\sqrt{(-\log_2(x))/2}$ for downregulated metabolites, where x is MYC/FLM (in c, e, g, i) or SYMB/ASYMB (in d, f, h, j).

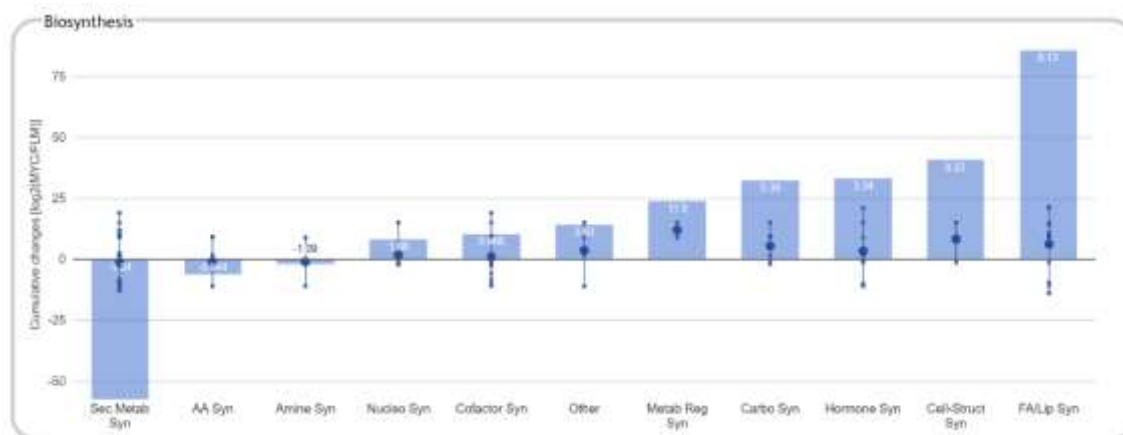


Figure 5: Cumulative changes of significantly differently produced compounds on the metabolisms of MYC samples, compared to FLM. MYC, fungal mycelium growing near the mycorrhizal protocorms; FLM, asymbiotic free-living mycelium. The functional classes are based on the MetaCyc pathway ontology (<https://metacyc.org/>) and the graph constructed using the Omics Dashboard (Paley *et al.*, 2017).

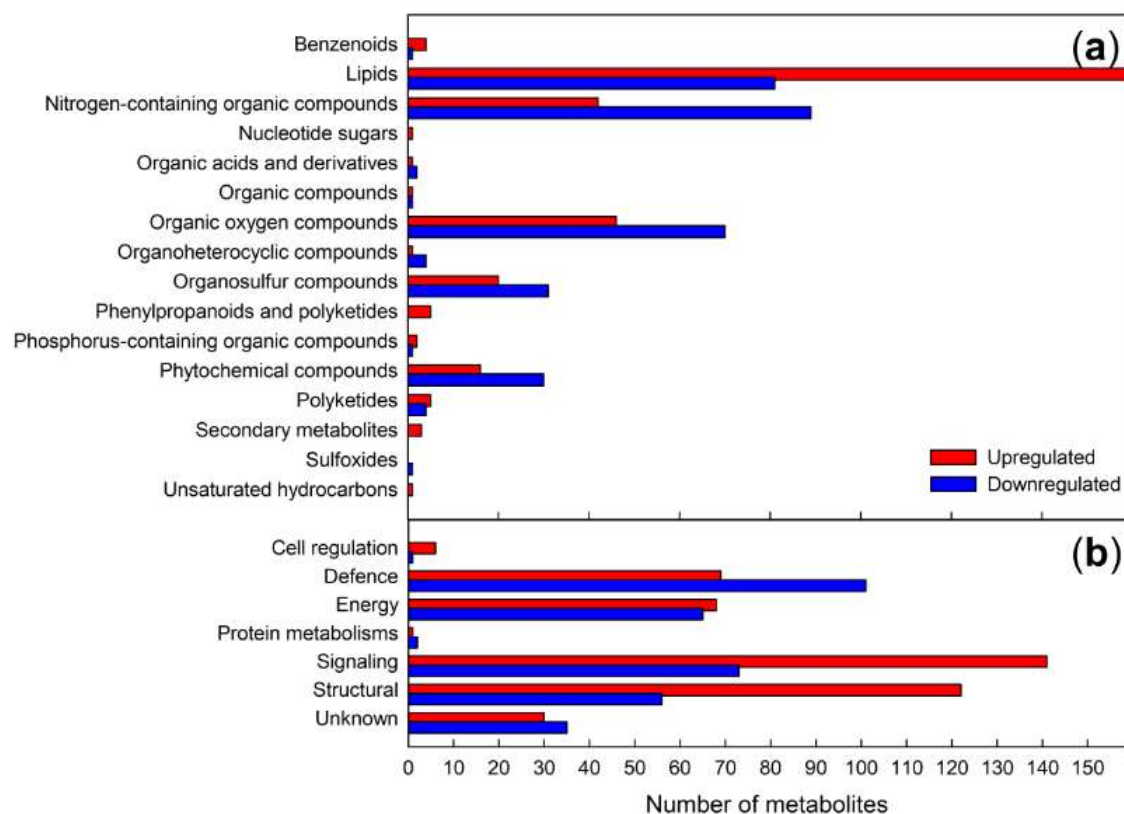


Figure 6: Changes of metabolites in the *T. calospora* mycelium. The number of metabolites grouped according to their (a) chemical taxonomy and (b) the biological functions of the up- (in red) and downregulated (in blue) metabolites in MYC samples, as compared to FLM. A comprehensive list is given in Table S1. The classification is based on KEGG, HMDB and Lipid Maps databases. Unknown organic compounds were classified based on the following priority of their atom compositions: S>P>N>O. For multifunction metabolites, the functions were added to different groups.

Supporting Information

Article title: **Metabolomic adjustments in the orchid mycorrhizal fungus *Tulasnella calospora* during symbiosis with *Serapias vomeracea***

Authors: Andrea Ghirardo, Valeria Fochi, Birgit Lange, Michael Witting, Jörg-Peter Schnitzler, Silvia Perotto, Raffaella Balestrini

The following Supporting Information is available for this article:

Fig. S1 Cumulative changes in lipid biosynthesis on the metabolisms of fungal mycelium (MYC) compared to free-living mycelium (FLM).

Table S1 Metabolomic annotation. (*attached*)

Table S2 Gene expression in *Tulasnella calospora*.

Table S3 Gene expression in *Serapias vomeracea*.

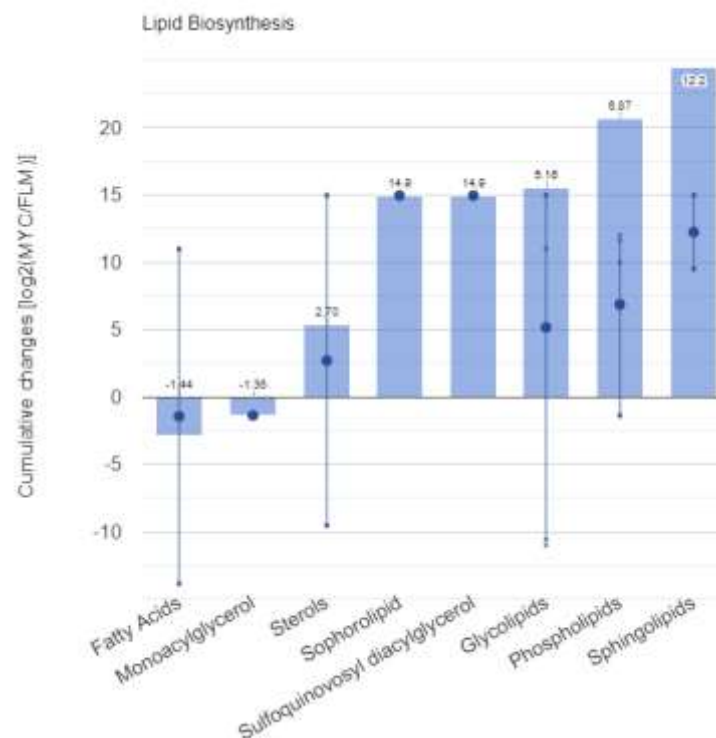


Fig. S1 Cumulative changes of significantly differently produced compounds involved in lipid biosynthesis on the metabolisms of MYC samples, compared to FLM. MYC, fungal mycelium growing near the mycorrhizal protocorms; FLM, asymbiotic free-living mycelium. The functional classes are based on the MetaCyc pathway ontology (<https://metacyc.org/>) and the graph constructed using the Omics Dashboard (Paley *et al.*, 2017).

Table S1 Excel file containing all the significant annotated molecular formulas of LC-MS measurements. (*online material*)

Table S2 Gene expression in *Tulasnella calospora* (Fochi et al., 2017a). Only genes significantly upregulated (FC>2, p-value<0.05) or downregulated (FC<0.5, p-value<0.05) in the comparison between symbiotic and asymbiotic conditions are reported.

Metabolism	Protein ID	Mean Read Count		SYMB/FLM comparison		Protein definition
		FLM	SYMB	Fold Change	FDR p-value*	
Glycerophospholipid /FA metabolism	53822	0.76	21.15	27.83	9.47E-09	Ca2+-independent phospholipase A2
	72491	10.37	185.29	17.87	4.07E-69	Myo-inositol-1-phosphate synthase
	25657	1.26	20.38	16.17	6.76E-08	Ca2+-independent phospholipase A2
	223254	5.91	33.53	5.67	4.22E-09	Lipid phosphate phosphatase
	244232	1.53	7.54	4.93	0.029349	Ca2+-independent phospholipase A2
	235323	46.03	222.55	4.83	1.45E-52	Lipid phosphate phosphatase
	69758	23.18	93.42	4.03	3.5E-11	Lysophospholipase
	113249	2.25	8.69	3.86	0.020451	Phosphate acyltransferase
	24893	19.26	56.86	2.95	6.86E-09	Lipid phosphate phosphatase
	34211	45.10	129.35	2.87	1.67E-08	Acyl-CoA synthetase
	25656	25.32	66.37	2.62	7.91E-09	Ca2+-independent phospholipase A2
	63963	14.25	33.85	2.38	0.000603	Predicted lipase
	241659	12.18	27.88	2.29	0.001902	Lysophosphatidic acid acyltransferase
	48469	83.70	185.09	2.21	1.03E-17	Acyl-CoA synthetase
	12116	30.59	66.71	2.18	1.27E-06	Phosphatidylinositol transfer protein
	65651	44.02	20.76	0.47	1.4E-05	Putative phosphoinositide phosphatase
	55914	42.26	19.11	0.45	8.4E-06	Predicted phospholipase
	16280	30.48	13.67	0.45	0.000304	3-oxoacyl CoA thiolase
	79164	64.39	28.44	0.44	8.25E-09	Peroxisomal long-chain acyl-CoA transporter
	218567	77.64	33.27	0.43	4.74E-11	Very-long-chain acyl-CoA dehydrogenase
	245357	31.93	13.53	0.42	0.000157	Enoyl-CoA hydratase
	227101	10.18	4.26	0.42	0.035275	Long chain fatty acid acyl-CoA ligase
	245109	11.19	4.30	0.38	0.015401	Enoyl-CoA hydratase
	131995	244.62	94.03	0.38	8.86E-10	3-oxoacyl CoA thiolase
	25831	75.79	27.28	0.36	3.33E-06	Enoyl-CoA isomerase
	244385	17.74	6.20	0.35	0.000882	Mitochondrial/plastidial beta-ketoacyl-ACP reductase
	240581	135.39	46.56	0.34	2.66E-14	Peroxisomal multifunctional beta-oxidation protein

Sphingolipid metabolism	243150	183.98	61.97	0.34	2.82E-08	Lipid phosphate phosphatase
	222821	49.06	16.50	0.34	0.001611	Triglyceride lipase-cholesterol esterase
	14918	52.55	16.97	0.32	2.16E-11	Acyl-CoA:diacylglycerol acyltransferase (DGAT)
	234265	85.95	27.57	0.32	0	Peroxisomal long-chain acyl-CoA transporter
	72780	62.38	15.32	0.25	5.32E-05	Ca2+-independent phospholipase A2
	243148	69.94	12.78	0.18	0	Lipid phosphate phosphatase
	191699	109.84	15.95	0.15	0	Predicted lipase
	244713	106.19	11.89	0.11	0	Acyl-CoA:diacylglycerol acyltransferase (DGAT)
	47248	465.71	29.63	0.06	0.000681	Phosphatidylserine decarboxylase
	18228	2.62	18.56	7.06	6.93E-06	Sphingosine N-acyltransferase.
	79587	12.31	52.25	4.24	2.43E-08	Sphingosine N-acyltransferase.
	18227	19.67	40.03	2.04	0.000892	Sphingosine N-acyltransferase.
	33445	40.84	4.17	0.10	0	Glucosylceramidase.
	27319	0.16	6.70	41.88	0.00235578	17 beta-hydroxysteroid dehydrogenase type 3. HSD17B3
	112707	0.61	22.49	36.87	1.51E-07	17 beta-hydroxysteroid dehydrogenase type 3. HSD17B3
	15520	5.31	66.76	12.57	2.16E-23	C-4 sterol methyl oxidase
	15617	7.84	84.02	10.72	3.16E-28	C-4 sterol methyl oxidase
	227917	3.01	23.74	7.89	1.24E-07	Hydroxymethylglutaryl-CoA reductase (NADPH).
	13385	18.94	104.95	5.54	4.54E-27	Sterol C5 desaturase
	97990	7.50	22.58	3.01	0.00048427	C-8.7 sterol isomerase
Steroid metabolism	37203	11.20	29.36	2.62	0.00206051	Hydroxymethylglutaryl-CoA reductase (NADPH).
	242907	22.80	57.27	2.51	3.03E-07	3-oxo-5-alpha-steroid 4-dehydrogenase.
	228549	13.32	29.56	2.22	0.0018794	3-keto sterol reductase
	245385	40.68	83.47	2.05	0.00927699	C-8.7 sterol isomerase
	20568	117.07	52.51	0.45	1.23E-07	START domain-containing proteins involved in steroidogenesis/phosphatidylcholine transfer
	76927	26.93	5.47	0.20	1.61E-08	Steroid reductase
	113659	122.22	22.29	0.18	0	Steroid reductase
	70959	1.95	52.49	26.92	1.74E-11	Terpenoid synthase
	22905	4.72	105.71	22.40	7.32E-20	Terpenoid synthase
	23789	3.16	29.45	9.32	9.57E-10	Terpenoid synthase
Terpenoid metabolism	145950	14.53	128.65	8.85	1.01E-40	Terpenoid synthase
	240449	8.90	27.97	3.14	4.75E-05	Cis-prenyltransferase
	214286	18.16	44.90	2.47	0.005619	Terpenoid synthase
	119731	15.07	31.99	2.12	0.010037	Phytoene dehydrogenase-related protein
	19151	66.18	29.56	0.45	7.26E-09	Prenyltransferase/squalene oxidase
	27794	11.86	4.01	0.34	0.015927	Peroxisomal phytanoyl-CoA hydroxylase

S-adenosyl-L-methionine metabolism	27796	137.39	45.42	0.33	0	Peroxisomal phytanoyl-CoA hydroxylase
	214327	41.06	7.31	0.18	6.86E-15	Terpenoid synthase
	228858	2.92	44.79	15.34	0.001399	SAM-dependent methyltransferases
	244998	32.75	166.80	5.09	7.45E-41	SAM-dependent methyltransferases
	72837	215.01	922.27	4.28	2.94E-39	S-adenosylmethionine synthetase
Chitin metabolism	21107	2.84	8.71	3.06	0.045065	SAM-dependent methyltransferases
	174258	1.32	27.07	20.51	1.76E-05	Chitin deacetylase
	26855	4.78	63.15	13.21	5.78E-12	Chitin deacetylase;
	107589	29.31	109.37	3.73	2.86E-18	Chitin deacetylase
	31299	11.46	23.48	2.05	0.0142	Chitin synthase
Histidine biosynthesis	33089	14.53	6.95	0.48	0.0257	Chitin deacetylase
	108905	17.67	144.87	8.201	5.7E-42	ATP phosphoribosyltransferase
	73648	15.20	70.89	4.663	1.77E-09	Histidinol dehydrogenase
	141375	12.16	39.12	3.217	5.88E-07	Phosphoribosylformimino-5-aminoimidazole carboxamide ribonucleotide (ProFAR) isomerase

* P-value = 0 indicates values <1E-70

Table S3 Expression of *S. vomeracea* contigs in symbiotic (SYM) and asymbiotic (ASYMB) protocorms. Contigs obtained in the *de novo* assembly were annotated by BlastX against the *A. thaliana* proteome.

Metabolism	Trinity Contig Name	Mean read count		SYMB/ASYMB comparison		<i>A. thaliana</i> Gene Id	Putative function in <i>A. thaliana</i>	score	e-value	percent identity
		SYMB	ASYMB	Fold Change	P-value					
Chitin metabolism	TRINITY_DN77284_c0_g1_i3	226.85	0.00	SYM*	1.58E-07	AT5G24090.1	Chitinase A	203	2.00E-20	69.2
	TRINITY_DN5745_c0_g1_i1	26.04	0.00	SYM*	0.015799	AT1G02360.1	Chitinase family protein	263	1.00E-28	63.4
	TRINITY_DN66370_c0_g1_i1	17.42	0.18	95.70	1.62E-06	AT5G24090.1	Chitinase A	786	5.00E-103	58.2
	TRINITY_DN62020_c0_g1_i1	45.79	1.40	32.60	1.21E-10	AT1G02360.1	Chitinase family protein	715	2.00E-92	64.1
S-adenosyl-L-methionine metabolism	TRINITY_DN95258_c0_g1_i1	10.59	0.03	343.40	0.005566	AT5G66430.1	SAM-dependent methyltransferases	369	3.00E-42	46.9
	TRINITY_DN44325_c0_g1_i1	21.46	0.62	34.79	4.62E-12	AT5G04370.2	SAM-dependent methyltransferases	103	2.00E-06	48.8
	TRINITY_DN75761_c2_g1_i1	19.99	0.98	20.45	1.42E-10	AT2G14060.1	SAM -dependent methyltransferases	287	8.00E-30	46.2
	TRINITY_DN67911_c0_g1_i2	93.74	5.30	17.68	3.2E-22	AT4G34050.1	SAM -dependent methyltransferases	639	2.00E-80	57
	TRINITY_DN75761_c1_g1_i1	5.52	0.43	12.77	0.014476	AT5G38020.1	SAM -dependent methyltransferases	292	6.00E-30	45.5
	TRINITY_DN75761_c0_g1_i3	16.36	1.43	11.44	5.58E-07	AT3G11480.1	SAM -dependent methyltransferases	273	4.00E-29	46.8
	TRINITY_DN75761_c2_g7_i1	11.85	1.09	10.82	2.8E-05	AT5G04370.2	SAM -dependent methyltransferases	120	4.00E-08	50.9
	TRINITY_DN75761_c1_g1_i3	16.55	2.62	6.31	0.001078	AT5G38020.1	SAM -dependent methyltransferases	298	1.00E-30	46
	TRINITY_DN67911_c0_g1_i1	86.46	17.49	4.94	2.52E-15	AT4G34050.1	SAM -dependent methyltransferases	635	1.00E-80	57
	TRINITY_DN75761_c2_g6_i1	8.50	1.87	4.55	0.041527	AT5G04370.1	SAM -dependent methyltransferases	123	2.00E-08	43.6

	TRINITY_DN69539_c1_g2_i2	29.21	8.28	3.53	0.001477	AT5G19530.1	SAM -dependent methyltransferases	1226	5.00E-167	68
	TRINITY_DN76586_c0_g1_i2	12.57	3.88	3.24	0.024737	AT2G43940.1	SAM -dependent methyltransferases	727	2.00E-93	61.8
	TRINITY_DN77952_c0_g2_i1	28.17	9.65	2.92	7.06E-05	AT4G00750.1	SAM-dependent methyltransferases	2064	0	63
	TRINITY_DN73756_c1_g13_i1	25.50	9.85	2.59	0.001217	AT4G10440.1	SAM -dependent methyltransferases	2293	0	68.6
	TRINITY_DN74865_c4_g1_i1	17.96	7.01	2.56	0.01841	AT5G64030.1	SAM -dependent methyltransferases	2213	0	66.2
	TRINITY_DN75661_c0_g2_i3	23.33	9.96	2.34	0.041245	AT4G26220.1	SAM -dependent methyltransferases	177	9.00E-17	67.4
	TRINITY_DN75699_c0_g12_i1	4.43	16.55	0.27	0.000675	AT2G32170.1	SAM -dependent methyltransferases	159	1.00E-13	61.9
	TRINITY_DN77162_c3_g1_i3	4.74	30.85	0.15	2.12E-12	AT4G00750.1	SAM -dependent methyltransferases	1078	3.00E-140	56.5
	TRINITY_DN76265_c0_g7_i1	0.74	6.63	0.11	0.007444	AT1G23360.1	SAM -dependent methyltransferases	101	3.00E-06	94.7

Note: SYM*, uniquely expressed in symbiotic conditions.